PPAR Research

# Patient-Specific Roles of PPARs and Related Signalling Pathways

Lead Guest Editor: Hongbao Cao
Guest Editors: Anastasia Nesterova and Sha Liu

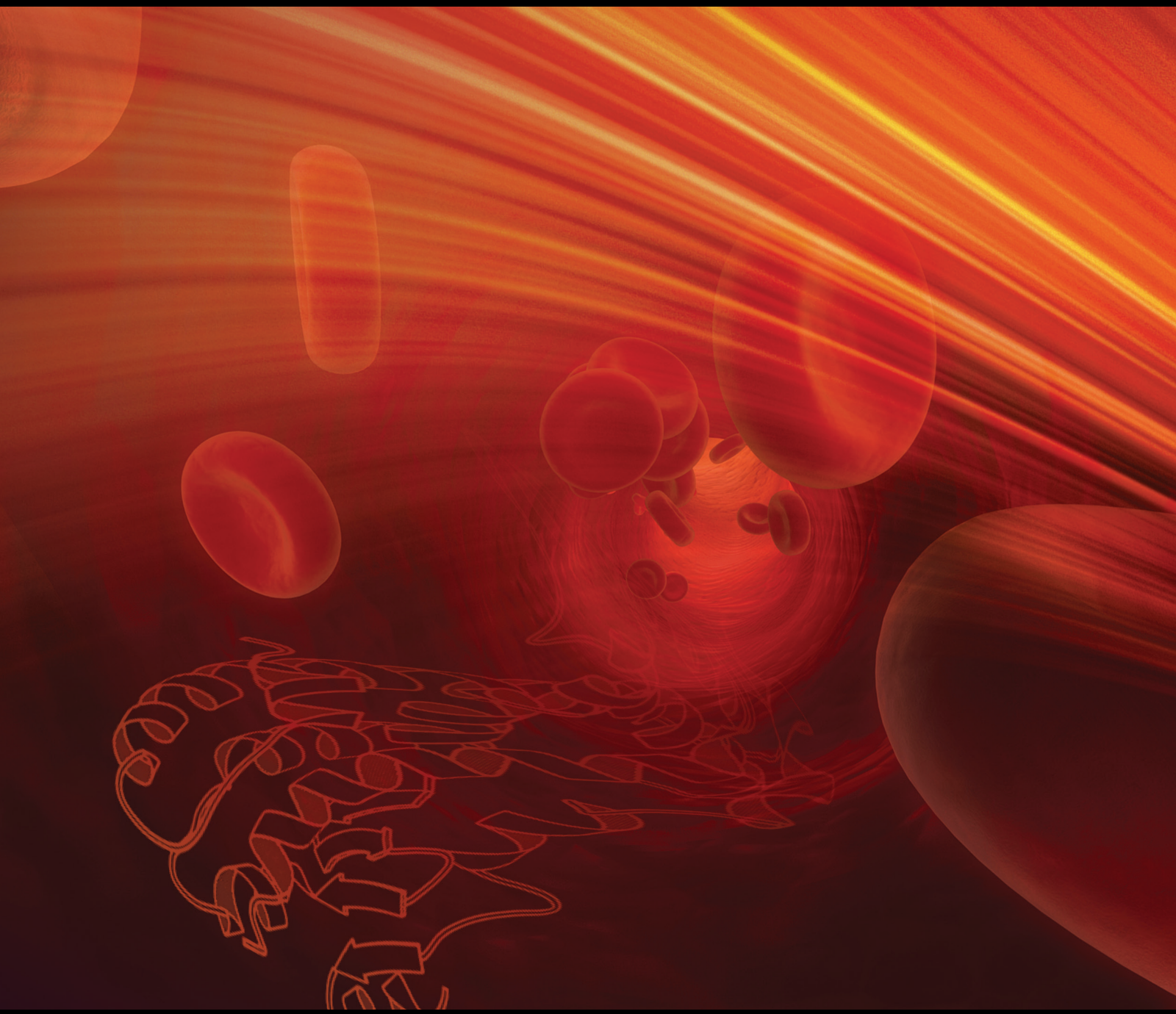

# Patient-Specific Roles of PPARs and Related Signalling Pathways

PPAR Research

# Patient-Specific Roles of PPARs and Related Signalling Pathways

Lead Guest Editor: Hongbao Cao
Guest Editors: Anastasia Nesterova and Sha Liu

# Contents

Hindawi
PPAR Research
Volume 2022, Article ID 5572258, 17 pages
https://doi.org/10.1155/2022/5572258

*Research Article*

# Comprehensive Analysis of Copy Number Variation, Nucleotide Mutation, and Transcription Level of PPAR Pathway-Related Genes in Endometrial Cancer

**Minghui Tang**,[1] **Jingyao Wang**,[2] **and Liangsheng Fan**[1]

[1]*Department of Obstetrics and Gynecology, The First Affiliated Hospital of Guangzhou Medical University, Guangzhou 510120, China*
[2]*Affiliated Cancer Hospital and Institute, Guangzhou Medical University, Guangzhou 510000, China*

Correspondence should be addressed to Liangsheng Fan; fanyi0606@163.com

Received 19 February 2021; Revised 1 December 2021; Accepted 17 December 2021; Published 13 January 2022

Academic Editor: Sha Liu



Endometrial cancer is a common malignant tumor in gynecology, and the prognosis of advanced patients is dismal. Recently, many studies on the peroxisome proliferator-activated receptor pathway have elucidated its crucial involvement in endometrial cancer. Copy number variation (CNA) and nucleotide mutations often occur in tumor tissues, leading to abnormal protein expression and changes in protein structure. We analyzed the exon sequencing data of endometrial cancer patients in the TCGA database and found that somatic changes in PPAR pathway-related genes (PPAR-related-gene) often occur in UCEC patients. Patients with CNA or mutation changes in the exon region of the PPAR-related-gene usually have different prognostic outcomes. Furthermore, we found that the mRNA transcription and protein translation levels of PPAR-related-gene in UCEC are significantly different from that of adjacent tissues/normal uterus. The transcription level of some PPAR-related-gene (DBI, CPT1A, CYP27A1, and ME1) is significantly linked to the prognosis of UCEC patients. We further constructed a prognostic predicting tool called *PPAR Risk score*, a prognostic prediction tool that is a strong independent risk factor for the overall survival rate of UCEC patients. Comparing to the typical TNM classification system, this tool has higher prediction accuracy. We created a nomogram by combining *PPAR Risk score* with clinical characteristics of patients in order to increase prediction accuracy and promote clinical use. In summary, our study demonstrated that PPAR-related-gene in UCEC had significant alterations in CNA, nucleotide mutations, and mRNA transcription levels. These findings can provide a fresh perspective for postoperative survival prediction and individualized therapy of UCEC patients.

## 1. Introduction

One of the most prevalent malignancies in the female reproductive system is uterine corpus endometrial carcinoma (UCEC), and its incidence has been rising in the past few years [1]. Most UCEC patients have a better prognosis after hysterectomy and adjuvant therapy. However, for advanced-stage patients, the benefit rate is less than 50% in current treatment strategies [2]. Therefore, it is still necessary to explore the pathogenesis of UCEC and treatments for advanced patients.

Peroxisome proliferator-activated receptors (PPARs) are transcription factors of the nuclear hormone receptor superfamily and play essential roles in the physiological and pathological processes of cells [3]. PPARs have been demonstrated to have an important function in the endometrial trophoblast in studies [4, 5]. Therefore, PPAR pathway-related genes (PPAR-related gene) also participate in the occurrence and development of UCEC. Some PPAR ligands have an antiproliferative activity against endometrial cancer [6]. Inhibition of PPAR$\gamma$ can promote the proliferation of endometrial cancer cells through the Bcl-2/caspase3 pathway [7].

Tumor somatic variation includes gene copy number alteration (CNA) and base mutation. Gene CNA includes amplification and deep deletion, which usually leads to

changes in the related protein expression. Intentional mutations of genes include missense mutation, truncating mutation, splice mutation, and inframe mutation. Gene mutations can cause changes in protein amino acids, thereby affecting their standard structure and function. We found 83% of serous endometrial carcinoma had PPAR-related gene somatic variation, while 48% of endometrioid endometrial carcinoma had PPAR-related gene somatic variation. This variation frequency is quite large, and further exploration is needed.

In this study, we conducted a comprehensive analysis of the CNA, nucleotide mutation, and transcription statuses of the PPAR-related gene in UCEC. Furthermore, we discovered that a substantial number of PPAR-related genes are associated with patient prognosis. As a result, a *PPAR risk score* was developed to predict the prognosis of UCEC patients. It contributes to a better understanding of the PPAR pathway's function in UCEC and allows for a more precise management of UCEC patients after surgery.

## 2. Materials and Methods

*2.1. PPAR Pathway-Related Gene Acquisition.* Sixty-nine PPAR-related genes were obtained from a gene set (KEGG PPAR signaling pathway) in the molecular signature database (MSigDB) [8]. The systematic name of this pathway is M13088. The specific details of the 69 PPAR-related genes investigated in this study are listed in Supplementary Table S1.

*2.2. Data Source and Study Population.* A total of 539 putative copy number alteration data and 248 mutation data from whole-exome sequencing for endometrial cancer samples in the TCGA database [9] were downloaded from cBioPortal [10]. The R package 'TCGAbiolinks' [11] was used to download the gene expression data and clinical data for 548 endometrial cancer samples in the TCGA-UCEC cohort. The Sankey plots used to display the samples' clinical information were drawn using the R package 'ggalluvial' [12].

*2.3. Pathway Enrichment Analysis.* The differentially expressed genes between the PPAR-related gene CNA/mutation altered group and the unaltered group were determined by using the R package 'edgeR.' Then, R package 'clusterProfiler' [13] was ulilized to perform gene set enrichment analysis (GSEA). The hallmark gene sets (h.all.v7.2.symbols.gmt) were downloaded from the MSigDB.

*2.4. Prognosis Analysis.* The overall survival (OS) and disease-free survival (DFS) of each group of patients were calculated using Kaplan-Meier and log-rank analyses.

*2.5. Immune Characteristic Analysis.* We used the CIBERSORT [14] algorithm to calculate the infiltration status of 22 immune cells in the TCGA-UECE cohort and compared the results in each group of patients. The neoantigens data and of the TCGA-UCEC cohort are from previously published articles. The total tumor-infiltrating lymphocytes (TIL) regional fraction data and the neoantigens data of the TCGA-UCEC cohort were obtained from an authoritative article [15].

*2.6. Prediction of Chemotherapy Response.* The R package 'pRRophetic' [16] and mRNA data were used to estimate each patient group's medication sensitivity. Among them, ridge regression was used to determine the samples' highest half-inhibitory concentration (IC50), and tenfold cross-validation was utilized to determine the accuracy.

*2.7. PPAR Risk Score Generation.* Through univariate and multivariate Cox regression analyses, the PPAR-associated gene most connected to patient prognosis was selected out. The linear combinational of the signature gene expression weighted by their regression coefficients was used to produce the *PPAR risk score* for each patient. The 'pheatmap' R package was used to visualize the expression of each gene in *PPAR risk score*. The survival rate was calculated using the Kaplan-Meier method, and its statistical significance was determined using the log-rank test.

*2.8. PPAR Risk Score Verification.* The prediction model based on *PPAR risk score* was tested using univariate and multivariate cox regression analyses to see if it was an independent prognostic factor. The time-dependent receiver operating characteristic curve (TDROC) in the 'survivalROC' [17] R package was used to examine *PPAR risk score*'s prediction ability at 1, 3, and 5 years.

*2.9. Statistical Analyses.* The clinical variables of different groups of patients were tested using Fisher's exact test or chi-square test. The Mann–Whitney *U* test or the Kruskal-Wallis test was utilized to compare the abundance of immune cell infiltration, neoantigens, and drug sensitivity between PPAR-related gene CNA/mutation altered and unaltered groups. $P < 0.05$ was considered statistically significant. The predictive nomogram was built with the R package 'rms' and Iasonos' guide [18]. R (version 4.0.3) or GraphPad Prism 6.0 was used for all statistical tests and visual analysis (GraphPad Software, USA).

## 3. Results

*3.1. The CNA Status of PPAR-Related Gene and Related Clinical Features in UCEC Patients.* We analyzed the CNA status of each PPAR-related gene in UCEC. In general, PPAR-related gene copy number changes are observed in 80% of patients with serous endometrial carcinoma (Figures 1(a)), which is much more than that of patients with endometrioid endometrial carcinoma (less than 20%). The PPAR-related gene most prone to copy number amplification are EHHADH, SLC27A1, ACOX1, ANGPLT4, and PLTP (Figures 1(b)). The PPAR-related gene most prone to copy number deletion are CPT1B and LPL. However, PPARA has undergone a large amount of copy number amplification and deletion. As shown in Figures 1(c), there is no difference in the PPAR-related gene CNA status among all age groups and histological grades. However, CNA of PPAR-related gene occurs more in serous type and III-IV TNM stage patients. To evaluate the relationship between the PPAR-related gene CNA status and the prognosis of UCEC, we divided patients into the PPAR-related gene altered and unaltered groups and compared their survival

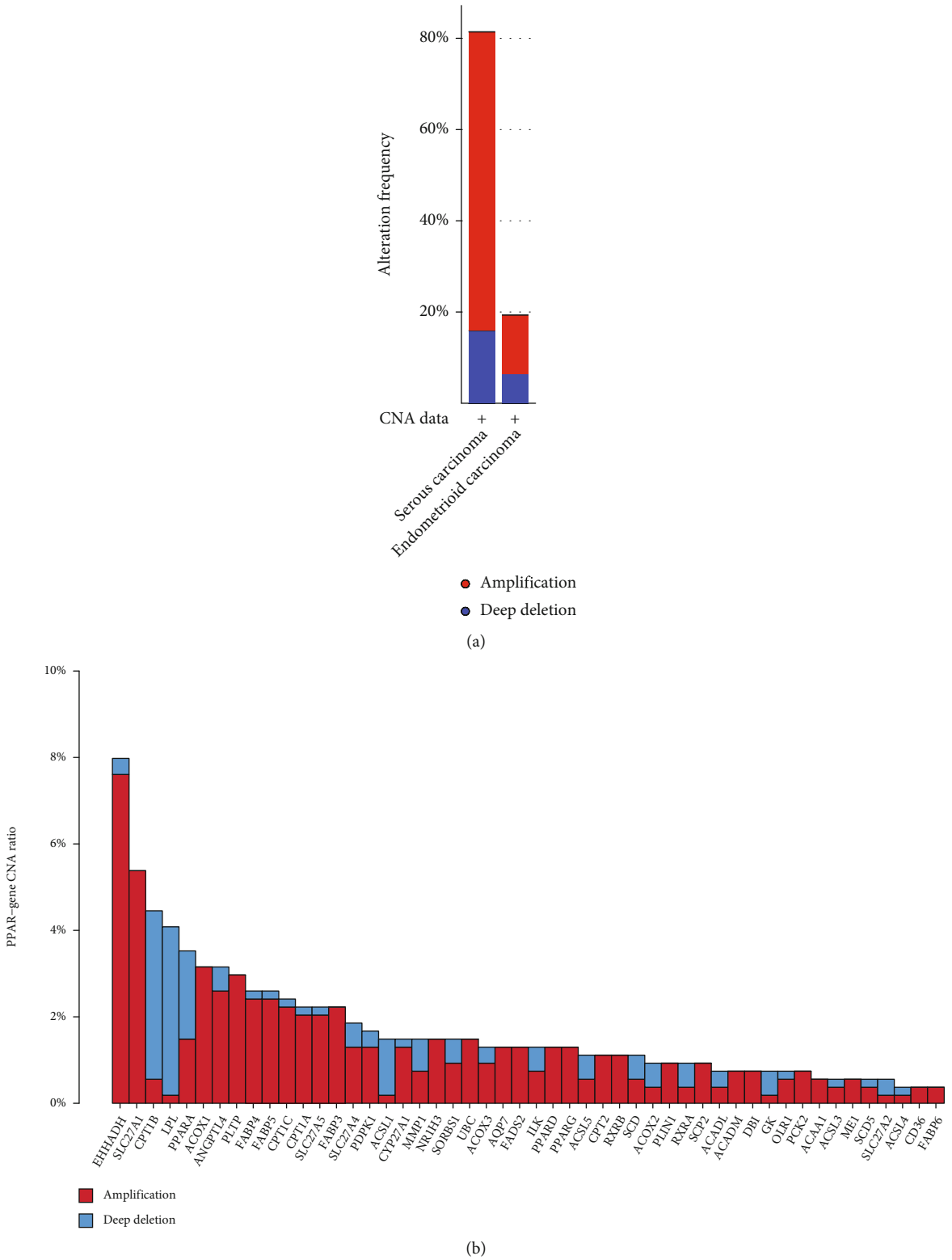


Figure 1: Continued.

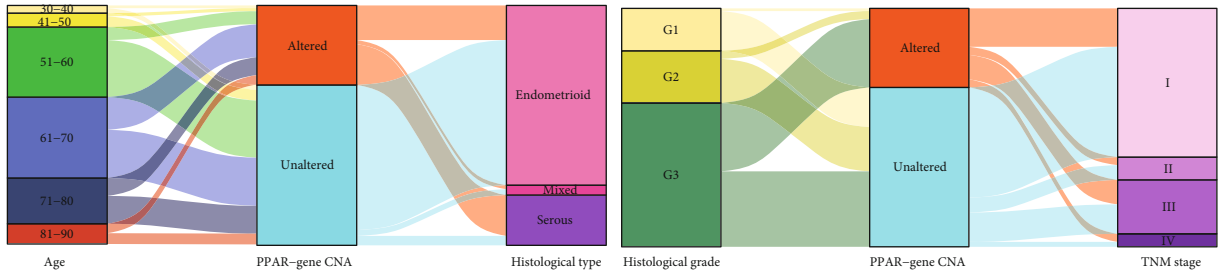


(c)

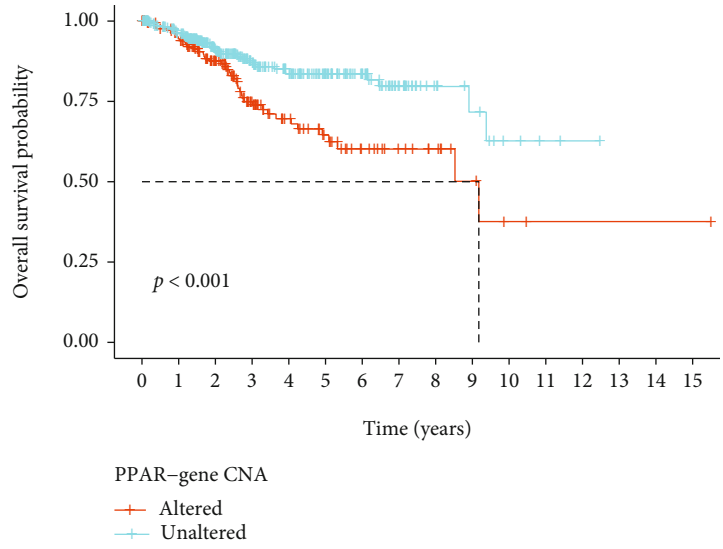


(d)

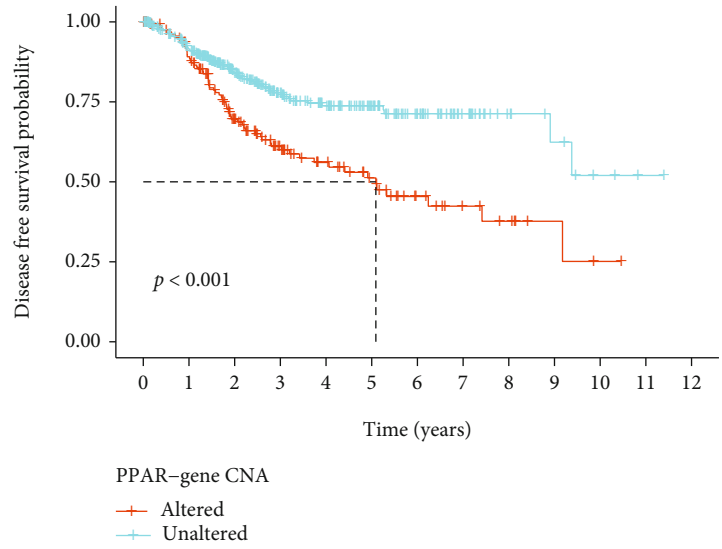


(e)

Figure 1: The CNA status of PPAR-related gene and related clinical features in UCEC patients. (a) The frequency of CNA alterations of PPAR-related gene in patients with different histological types. (b) The CNA type ratio of each PPAR-related gene. (c) Sankey plots show the clinical information of PPAR-related gene CNA and non-CNA patients. Kaplan-Meier curves show the correlation between PPAR-related gene CNA status and overall survival (d) or disease-free survival (e) probability of UCEC patients.

probabilities. When PPAR-related gene CNA occurs, the probability of OS and DFS of patients was lower than that of CNA unaltered patients (Figures 1(d) and 1(e)).

*3.2. The Mutation Status of PPAR-Related Gene and Related Clinical Features in UCEC Patients.* In a similar way, we also analyzed the mutation status of each PPAR-related gene in

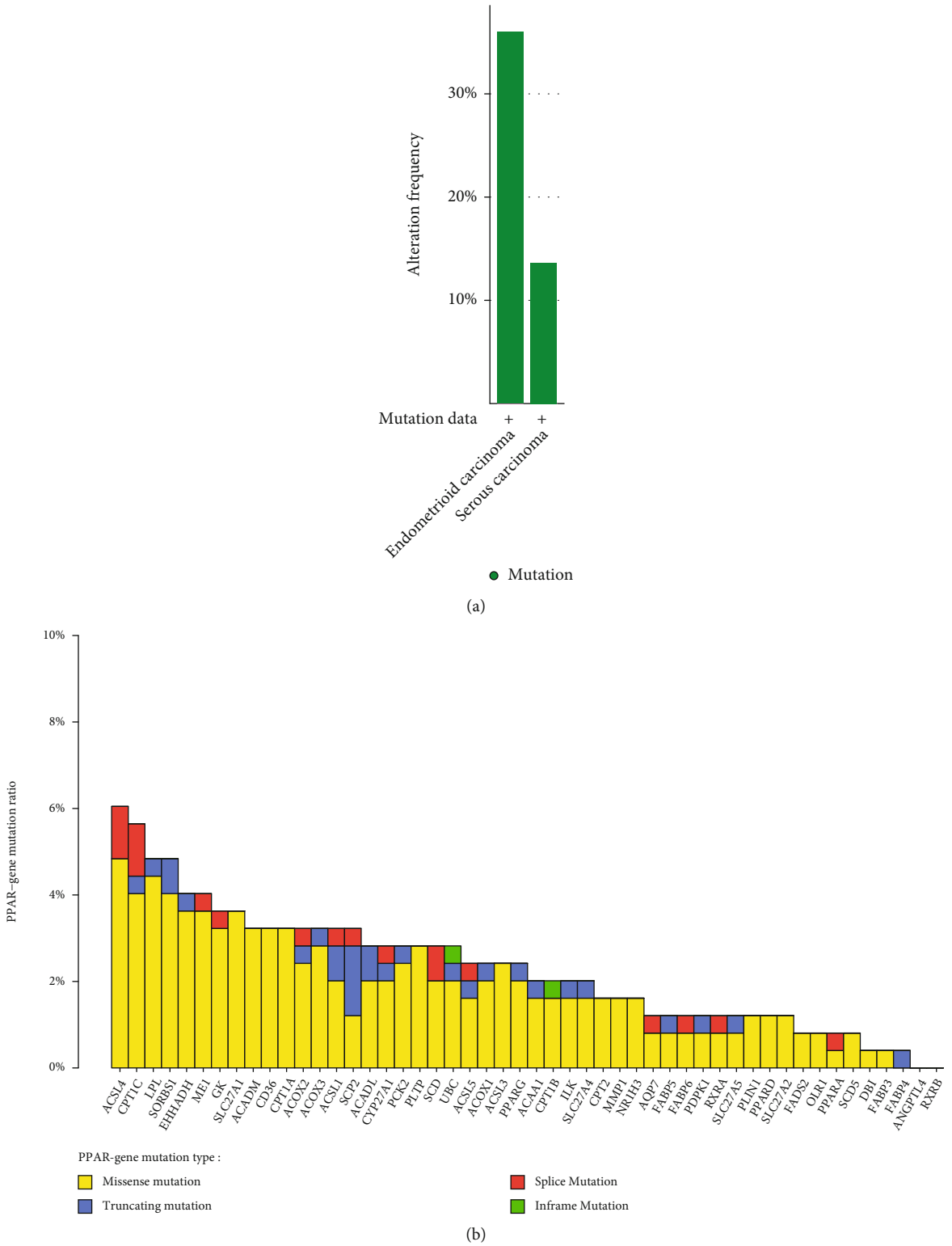


Figure 2: Continued.

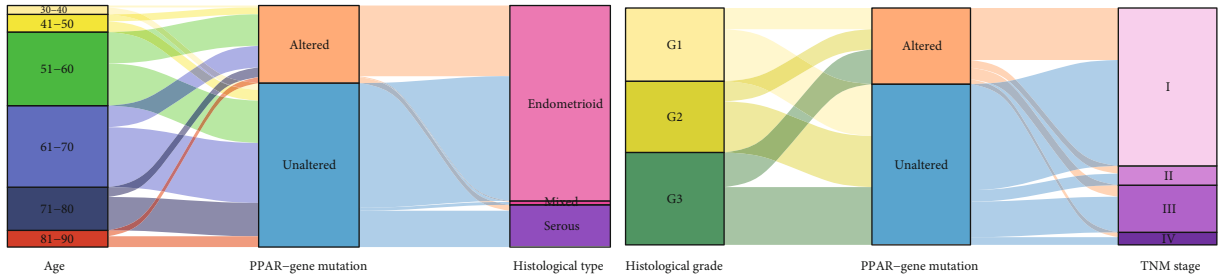


(c)

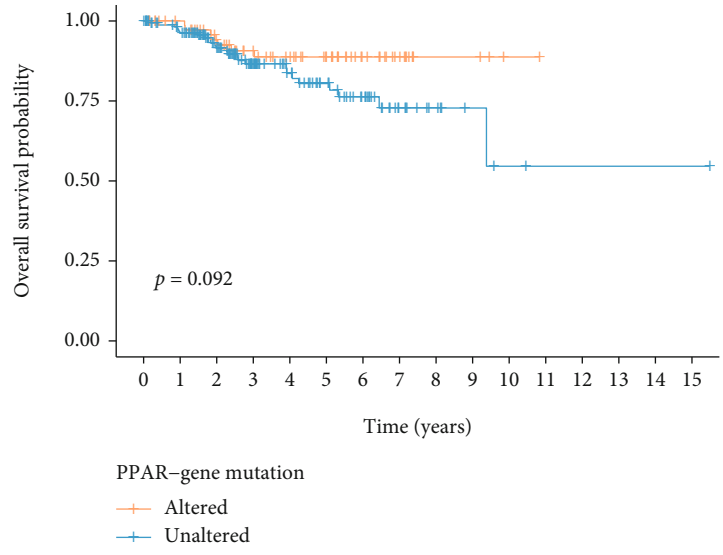


(d)

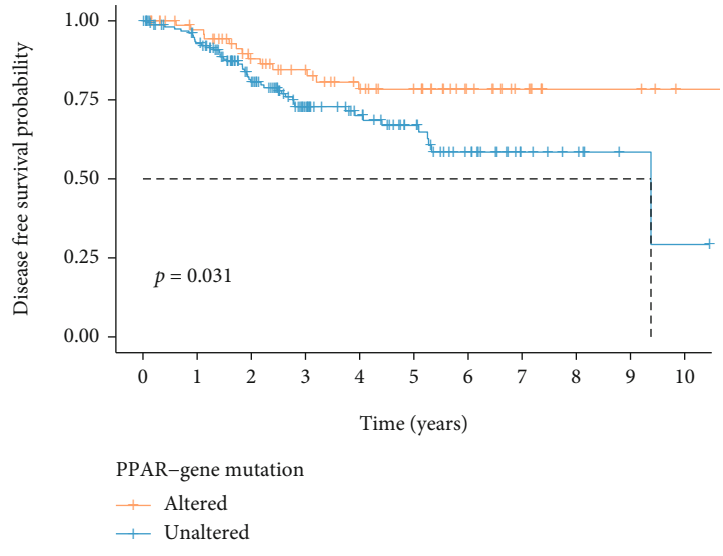


(e)

Figure 2: The mutation status of PPAR-related gene and related clinical features in UCEC patients. (a) The frequency of mutation alterations of PPAR-related gene in patients with different histological type. (b) The mutation type ratio of each PPAR-related gene. (c) Sankey plots shows the clinical information of PPAR-related gene mutated and nonmutated patients. Kaplan-Meier curves show the correlation between PPAR-related gene mutation status and overall survival (d) or disease-free survival (e) probability of UCEC patients.

UCEC. In general, the mutation of the PPAR-related gene is higher in endometrioid endometrial carcinoma than in serous endometrial carcinoma (Figure 2(a)). Commonly mutated PPAR-related genes are ACSL4, CPT1C, LPL, and SORBS1 (Figure 2(b)). A fascinating phenomenon is that EHHADH and LPL undergoes high copy number alterations and have high-frequency mutations in UCEC. As shown in Figures 2(c), there is no difference in the mutation

probability of PPAR-related gene among all age groups and histological grades. Similarly, we divided patients into the PPAR-related gene mutated and nonmutated groups and compared their survival probabilities. Kaplan-Meier analysis of OS and DFS showed that the prognosis of patients with PPAR-related gene mutation was better than that of nonmutated patients (Figures 2(d) an(d) 2(e)).

*3.3. Comparison of Transcriptomic Traits between PPAR-Related Gene Altered and Unaltered Patients.* To further analyze the potential biological changes in UCEC after PPAR-related gene CNA or mutation, we used the hallmark gene sets (h.all.v7.2.symbols.gmt) from the 'MSigDB' to perform the GSEA between the PAPP-gene altered and nonaltered groups. The full 50 pathways/gene sets enriched with were presented in the Supplementary Materials—GSEA results. Based on the adjusted $P$ value and normalized enrichment score, we selected the five pathways with the most significant changes for display. The results of GSEA showed that E2F TARGETS, G2M CHECKPOINT, and INTERFERON ALPHA RESPONSE pathways were significantly upregulated in the PPAR-related gene CNA altered group. In contrast, ESTROGEN RESPONSE pathways were significantly downregulated (Figure 3(a)). When PPAR-related gene mutations occur in UCEC patients, in addition to E2F TARGETS, G2M CHECKPOINT, and INTERFERON GAMMA RESPONSE pathways, the ALLOGRAFT REJECTION and INFLAMMATORY RESPONSE pathways were also significantly activated (Figure 3(b)).

*3.4. Association between the PPAR-Related Gene Status and Tumor Immune Characteristics.* Through the analysis of the CIBERSORT algorithm, we found that the tumor microenvironment of UCEC patients with PPAR-related gene CNA has changed. Nevertheless, in UCEC patients with PPAR-related gene mutation, these changes were more prominent. In PPAR-related gene CNA patients, the enrichment of $CD8^+$ T cell, Treg, and M1 type macrophage was reduced (Figure 4(a)). The total TIL fraction score did not change, but patients in the CNA group had fewer neoantigens (Figure 4(b)). In the PPAR-related gene mutation group, CD8+ T cell, T helper, and M1 type macrophage infiltration increased (Figure 4(c)). Also, in the PPAR-related gene mutation group, the total TIL immersion score increased, and more neoantigens (Figure 4(d)).

*3.5. Prediction of Chemotherapy Therapy Outcomes in Patients with Different PPAR-Related Gene Status.* UCEC patients use chemotherapy drugs for adjuvant treatment after surgery. In order to explore whether PPAR-related gene CNA and mutation status influence chemotherapy, we used the R package 'pRRophetic' to evaluate the patient's (TCGA-UCEC cohort) sensitivity to the drugs. We selected four chemotherapy drugs commonly used in UCEC patients and predicted their IC50 for the PPAR-related gene alternated and nonaltered patients (Supplementary Figure S1). Cisplatin is a commonly used chemotherapy drug for patients with endometrial cancer. Through bioinformatics prediction, we found that patients with CNA and mutations of PPAR-related genes may be more sensitive to cisplatin (low IC50). Besides, we found that PPAR-related gene CNA patients were more sensitive to paclitaxel ($P < 0.001$) than unaltered patients but less sensitive to docetaxel ($P < 0.001$). There was no difference in sensitivity to doxorubicin between the two groups. We did not find any statistical difference in the above three drugs' sensitivity between patients with PPAR-related gene mutations and those without mutations.

*3.6. The Transcription and Protein Expression of PPAR-Related Gene in UCEC Is Different from Normal Endometrium.* The CNA and mutation of genes ultimately perform biological functions by differentially changed RNA transcription and protein expression. We used RNA-seq and CPTAC (clinical proteomic tumor analysis consortium) protein expression data from UCEC patients and normal endometrium for further analysis. Firstly, we used principal component analysis (PCA) to describe the dimensionality reduction features of 50 PPAR-related genes. In the two-dimensional and three-dimensional PCA analysis results (Figure 5(a)), we found that PPAR-related gene can well distinguish UCEC (TCGA-UCEC-tumor), paratumor tissue (TCGA-UCEC-normal), and normal endometrium (GTEx-uterus). The results show that the expression of PPAR-related gene in these three tissues has different expression characteristics. We describe the transcription level of each gene in the PPAR-related gene set between UCEC paratumor tissues, endometrioid UCEC, and serous UCEC (Figure 5(b)). Similarly, we also analyzed the protein translation level of each PPAR-related gene (Supplementary Figure S2). The results showed that the RNA expression of EHHADH decreased in endometrioid UCEC and significantly increased in serous UCEC. But at the level of protein expression, we found that EHHADH was significantly increased in both types of UCEC. The LPL gene has high copy number deletions and missense mutations. Consistent with this, we have also observed a decrease in its transcriptome and proteome in UCEC. For other genes, some of them have the same trend in the transcriptome and proteome, but some are inconsistent.

*3.7. The Transcription of PPAR-Related Gene Is Related to the Prognosis of UCEC Patients.* We performed univariate Cox regression analysis using TCGA-UCEC mRNA sequencing data and clinical data to investigate the relationship between the expression of PPAR-related genes and patient prognosis. As shown in Figure 6(a), we discovered seven genes that are substantially related to UCEC patient prognosis ($P < 0.05$, HR < 1 or HR > 1) and passed the proposed bootstrap test. For dimension reduction, the seven robust prognostic genes were subjected to multivariate Cox regression analysis. We discovered that the model composed of four genes functioned optimally (Figure 6(a)). Among them, CYP21A1 has a hazard ratio of less than one, implying that individuals who overexpress CYP21A1 live longer. Three genes (DBI, CPT1A, and ME1) with hazard ratios greater than one, on the other hand, have the opposite implication. We created a scoring system called *PPAR risk score* to

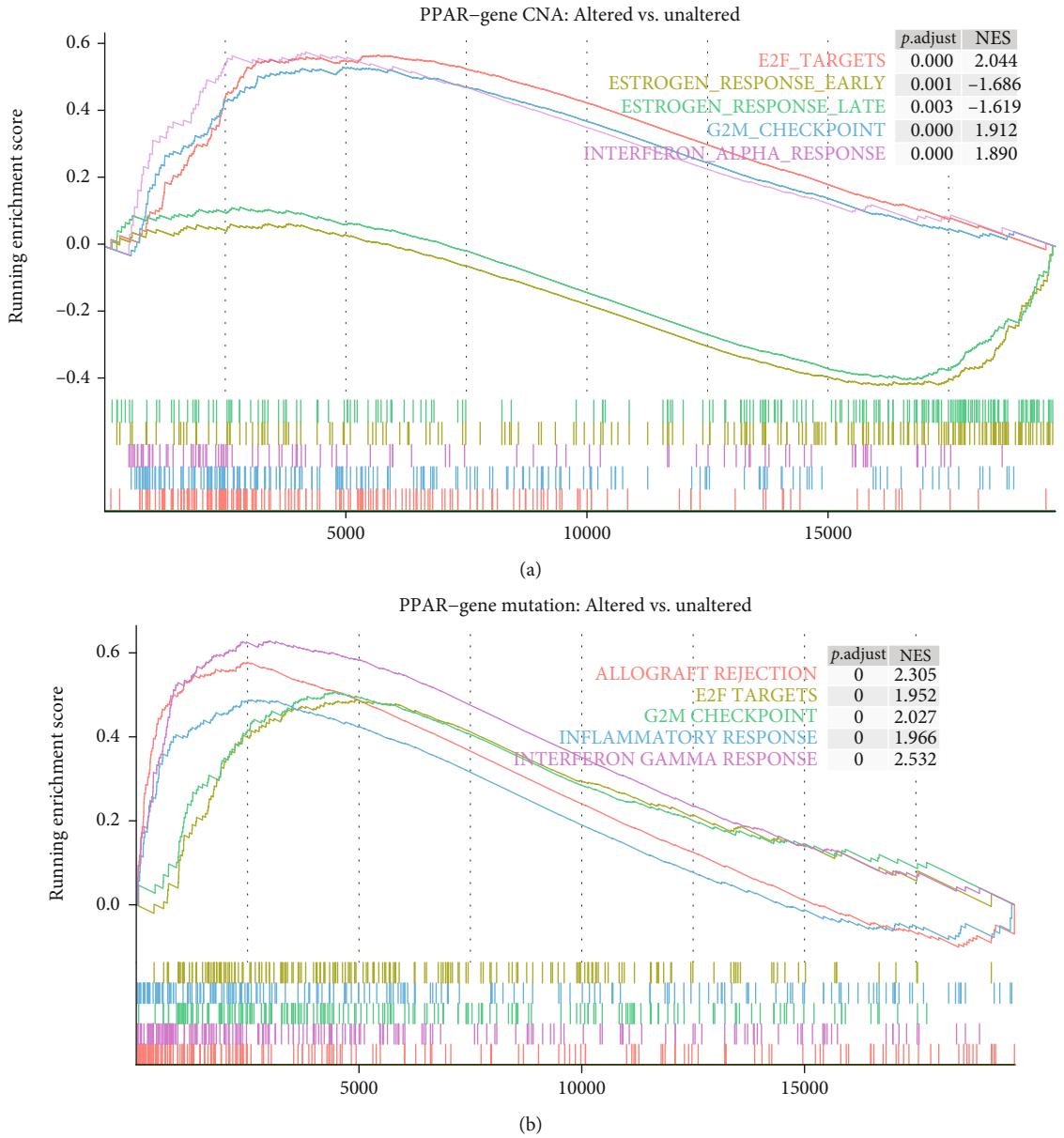


Figure 3: GSEA analysis between PPAR-related gene altered patients and unaltered patients. The five most significantly changed pathways in the PPAR-related gene CNA patients (a) and the PPAR-related gene mutation patients (b). *P*.adjust: adjusted *P* value; NES: normalized enrichment score.

predict the prognosis of UCEC patients based on the correlation coefficient of each gene.

$$\text{PPAR Risk score} = 0.54 * \text{Exp}_{\text{DBI}} + 0.41 * \text{Exp}_{\text{CPT1A}} - 0.35 * \text{Exp}_{\text{CYP27A1}} + 0.20 * \text{Exp}_{\text{ME1}}. \quad (1)$$

We estimated the *PPAR risk score* for each UCEC patient. Patients were divided into two groups (high risk and low risk) according on their *PPAR risk score*, using the cohort's median as the cut-off value. Figure 6(c) illustrates the distribution of *PPAR risk score* and patient survival status. The relative mRNA levels of such four genes between the two patient groups are depicted in Figure 6(d).

*3.8. Independent Prognostic Value of the PPAR Risk score.* The PPAR risk score is then compared to patient clinical data. The *PPAR risk score* was found to be a major independent risk factor for the overall survival rate of UCEC patients in both univariate and multivariate Cox regression analyses (Figure 7(a)). The Kaplan–Meier curve revealed that patients in the high-risk group had a significantly reduced survival rate (Figure 7(b)). The *PPAR risk score* outperformed the age, TMN stage, and pathological grade of UCEC patients in a one-year, three-year, and five-year ROC analysis (Figure 7(c)). These data imply that the *PPAR risk score* is

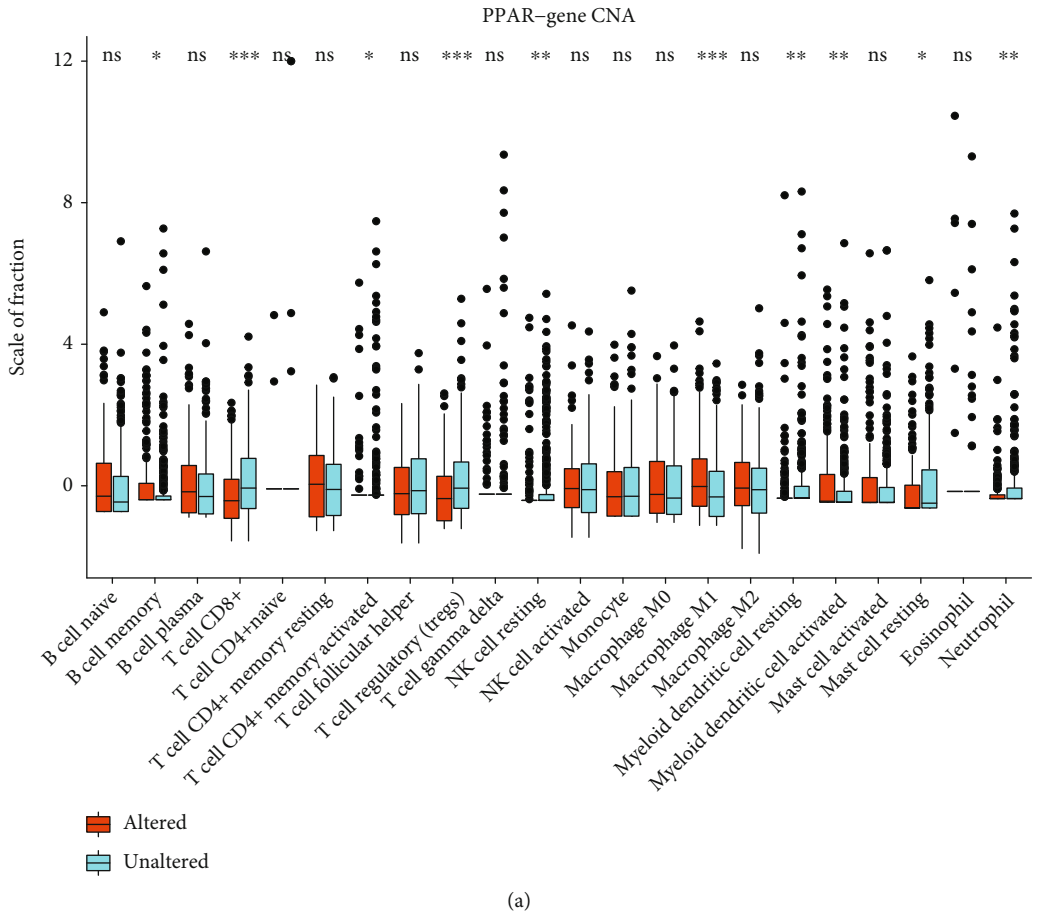


(a)

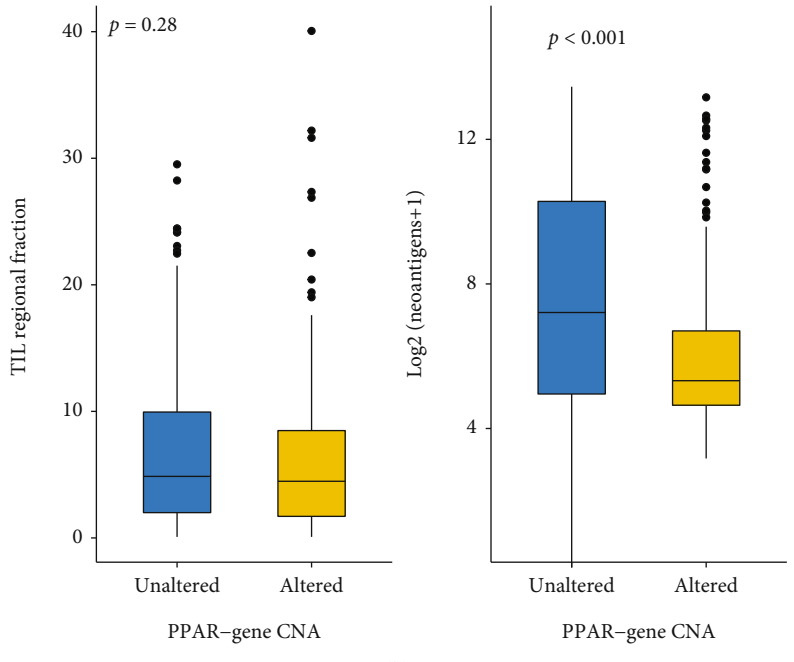


(b)

Figure 4: Continued.

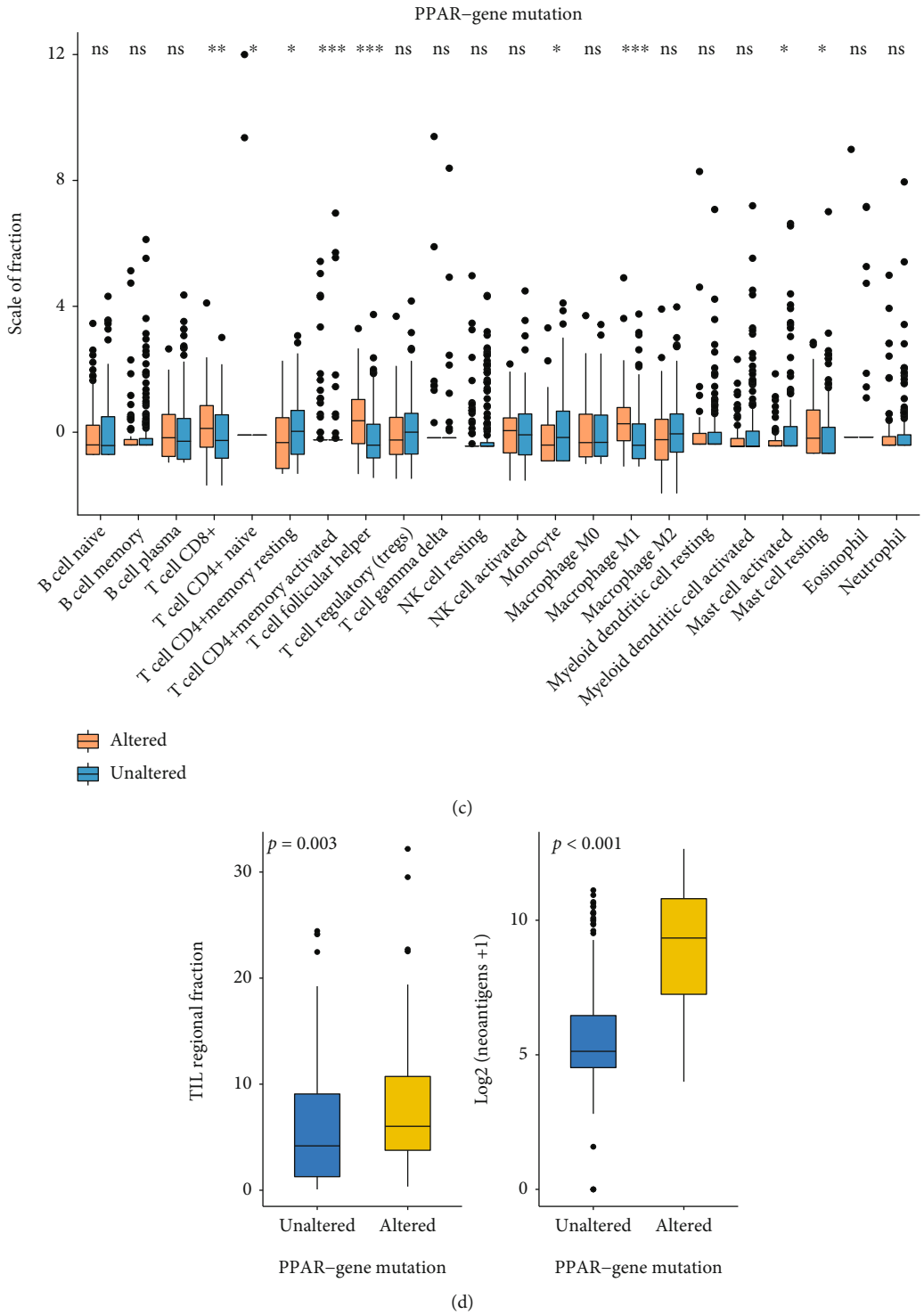


Figure 4: Tumor immune characteristics of patients with PPAR-related gene altered patients and unaltered patients. The relative abundance of tumor-infiltrating leukocytes (TILs) and neoantigens grouped by PPAR-related gene CNA status (a, b) and PPAR-related gene mutation status (c, d) in UCEC.

a distinct prognostic factor that may be more effective in predicting patient outcome than existing clinical measures.

*3.9. Develop a Prognostic Nomogram Based on PPAR Risk Score.* We developed a nomogram that integrates *PPAR risk score* and clinical prognostic factors to predict patients' 3- and 5-year survival rates (Figure 8(a)) in order to improve prognosis accuracy and ease clinical use. The patient's prognosis can be calculated using the sum of each factor's contribution scores. Figure 8(b) shows that

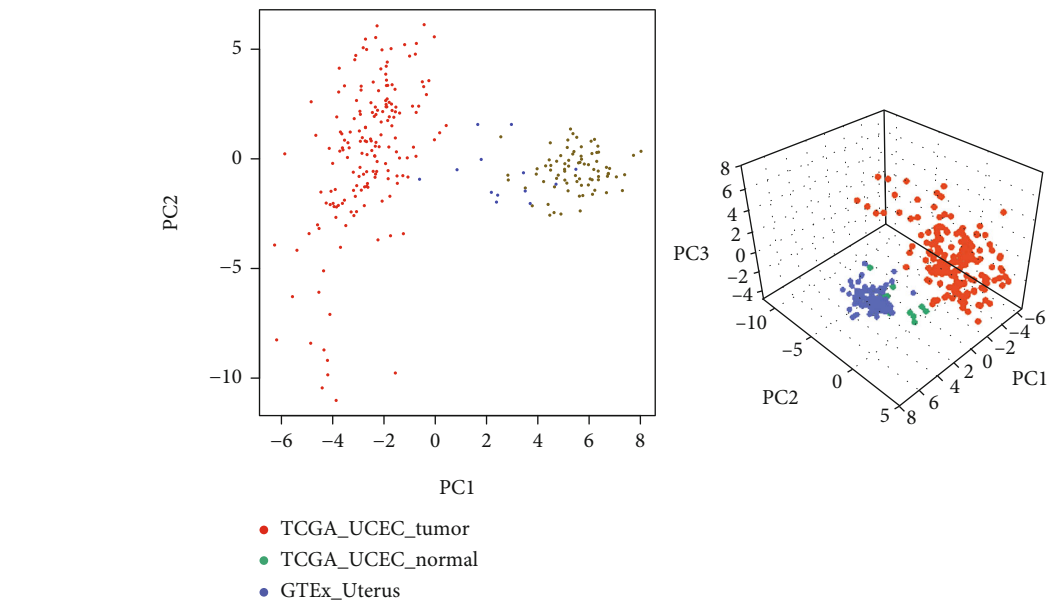


(a)

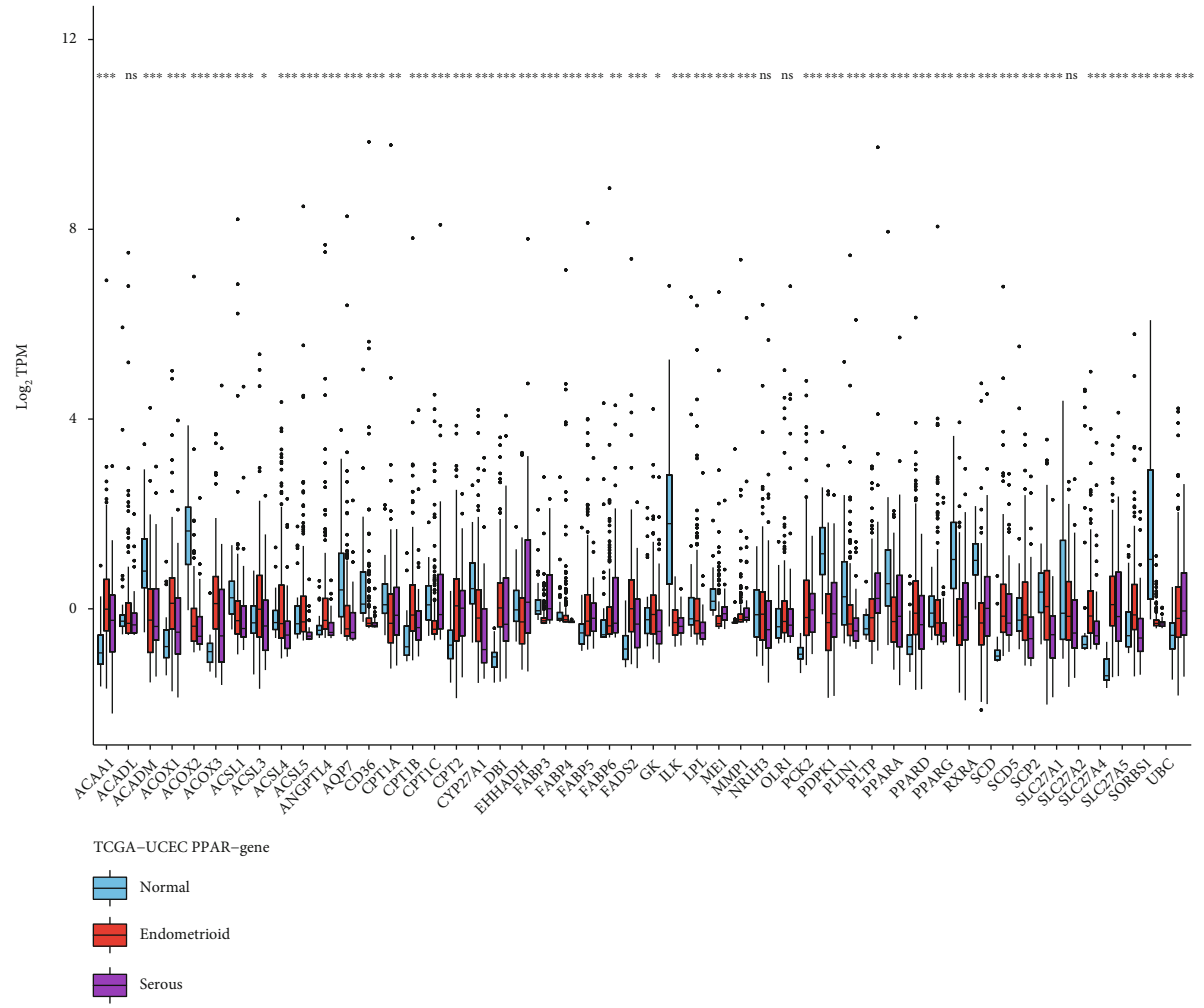


(b)

Figure 5: The transcription and protein expression analysis of PPAR-related-gene in UCEC. (a) The two-dimensional and three-dimensional PCA analysis results for PPAR-related-gene transcriptome. (b) The transcription level of each PPAR-related-gene between UCEC para-tumor tissues, endometrioid UCEC, and serous UCEC.

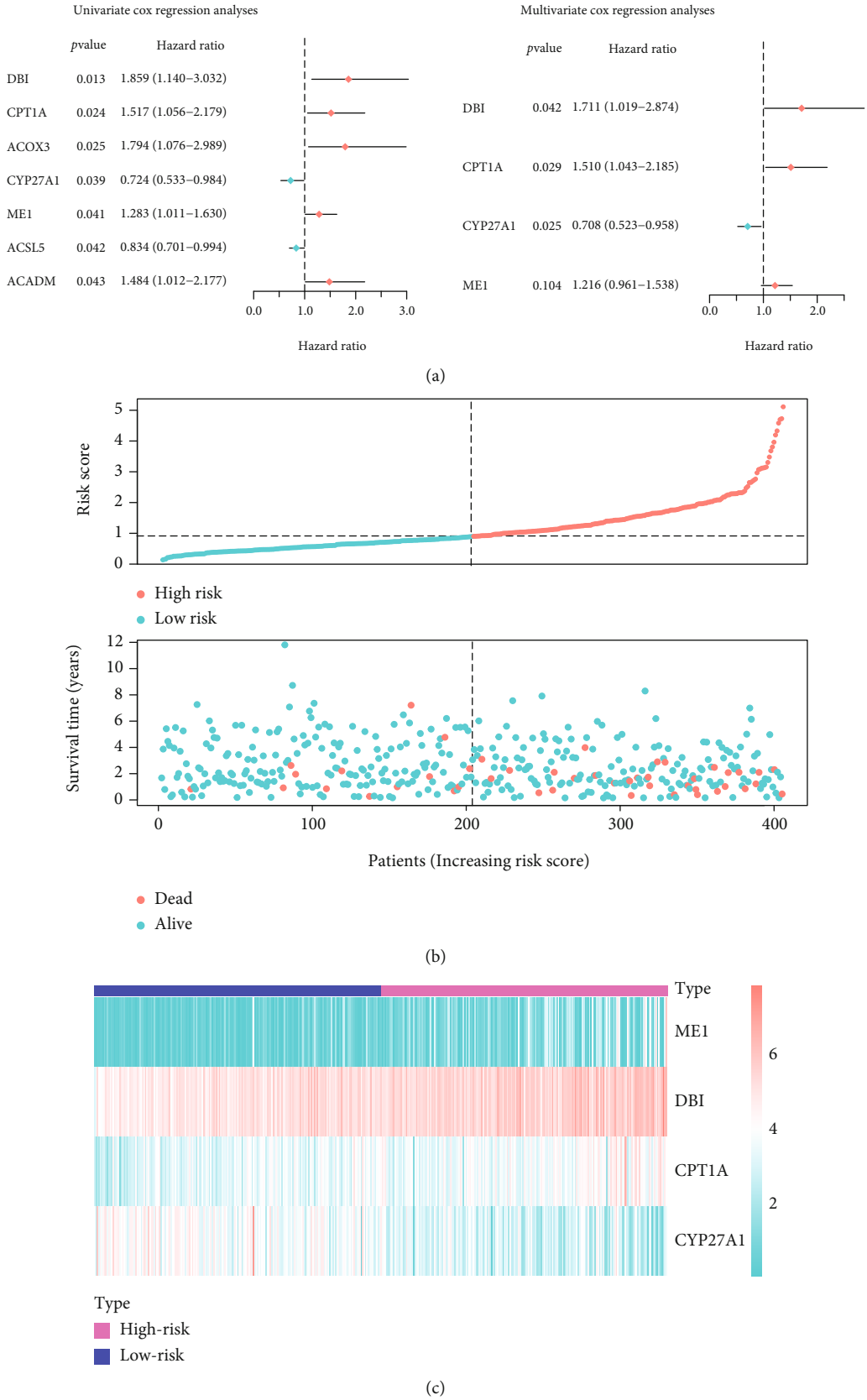


Figure 6: The construction of *PPAR risk score*. (a) Forest plot of the univariate and multivariate Cox regression analyses with the expression of PPAR-related gene. (b) The distribution of *PPAR risk score* and the survival status of patients with different scores. (c) Heatmap of the expression profiles of the *PPAR risk score* gene panel.

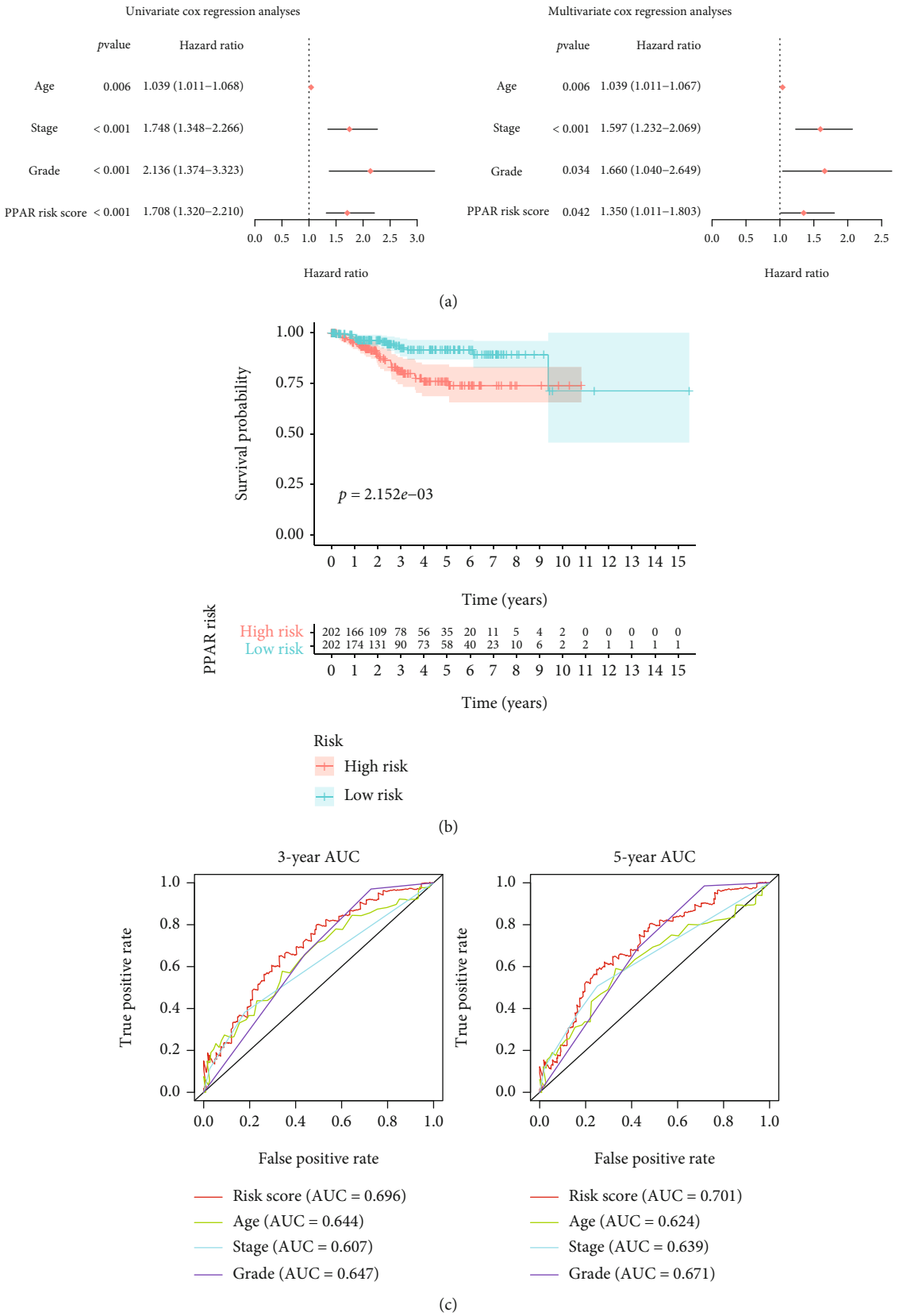


Figure 7: Verification of the *PPAR risk score's* independent prognostic value. (a) Forest plots of univariate and multivariate Cox regression analysis involving the *PPAR risk score* and clinical variables. (b) Overall survival Kaplan-Meier curves for patients in the high-risk and low-risk groups. (c) Curves of time-dependent receiver operating characteristic at one, three, and five years. AUC: area under curve.

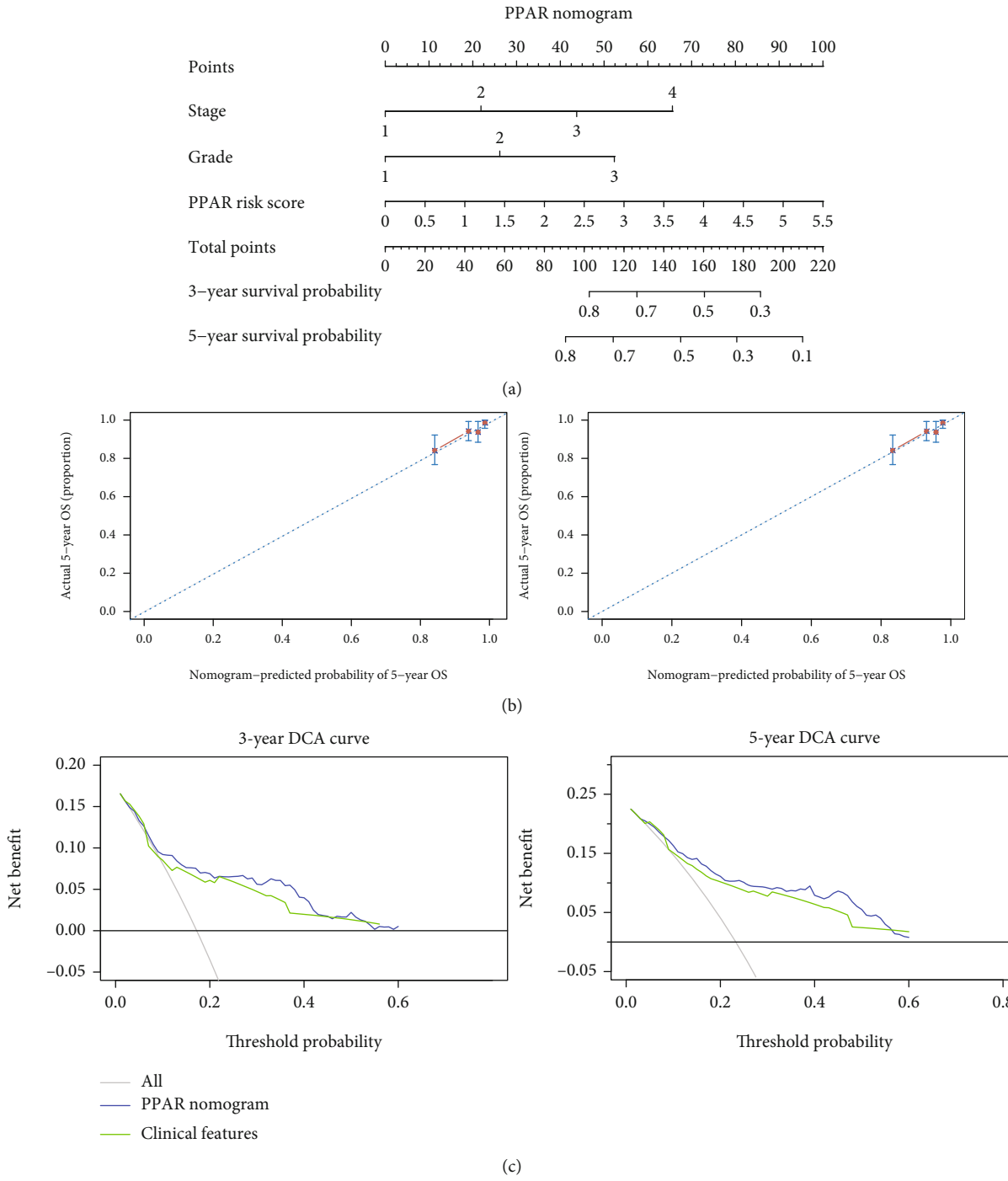


Figure 8: The establishment and verification of a nomogram based on the *PPAR risk score*. (a) A nomogram for estimating individual UCEC patients' 3- and 5-year survival chances. (b) Plots show how the nomogram was calibrated using the PPAR risk score in terms of consistency between anticipated and observed 3- and 5-year outcomes. (c) Nomogram decision curve studies for 3- and 5-year risks.

our nomogram outperforms an ideal model after three and five years of calibration. The clinical utility of our nomogram greatly outweighed the clinical features, according to the decision curve analysis (Figure 8(c)). It was discovered that using the *PPAR risk score* in combination with clinical features to predict prognosis could benefit more patients.

## 4. Discussion

Endometrial cancer is one of the primary gynecological malignancies globally. Its high-risk factors include disease stage, tumor size, grade, histological type, myometrial invasion, and lymph node metastasis [19]. It usually occurs in postmenopausal women, and the prognosis of late UCEC

is very poor, which requires our focus. Like other cancers, the incidence and progression of UCEC also entail complicated molecular pathways [20]. Studies have demonstrated that the PPAR pathway plays a key role in UCEC [4–7]. Through bioinformatics research, we detected a substantial number of somatic mutations in the PPAR pathway-related genes in UCEC. Therefore, it is crucial to comprehensively examine the CNA and mutation status of PPAR pathway-related genes in UCEC.

This study found that a large proportion of PPAR-related gene CNAs were observed in patients with serous carcinoma. On the other hand, PPAR-related gene mutation frequency is higher in endometrioid endometrial cancer but not serous carcinoma. The PPAR-related gene most prone to CNA amplification is EHHADH, one of the four enzymes of the peroxisomal beta-oxidation pathway [21]. EHHADH can promote cisplatin resistance in bladder cancer cells [22]. Highly expressed EHHADH may play a similar function in UCEC, which requires more in-depth research.

To further analyze the biological changes in UCEC after PPAR-related gene CNA and mutation, we performed GSEA analysis. To further analyze the biological changes of UCEC when the PPAR-related gene somatic mutation occurs, we conducted pathway analysis. It can be concluded that when a somatic mutation of the PPAR-related gene occurs in UCEC, cell cycle-related pathways will be activated. Such as the E2F pathway and G2/M DNA damage checkpoint-related proteins. Gene expression in response to the interferon-gamma (IFN$\gamma$) pathway is significantly upregulated, common in other tumors [23]. Immune checkpoint blockade therapy can lead to upregulation of IFN$\gamma$ and ultimately eliminate tumor cells. However, IFN$\gamma$ signal can also induce tumor ischemia and homeostasis program, and the result is tumor clearance or tumor escape [24]. Therefore, the significant activation of IFN$\gamma$ associated with PPAR-related gene somatic mutations in UCEC is a complicated research direction.

In the survival analysis, we found that PPAR gene CNA patients' survival time was significantly reduced compared with patients with unaltered CNA. On the other hand, compared with unaltered patients, PPAR-related gene mutation patients' survival time increased significantly. It is also an important conclusion we reached. It indicates that the somatic mutation status of PPAR-related gene may be an ideal prognostic predictor of UCEC. Clinicians can perform PPAR-related gene exon detection through the tumor tissue removed during a hysterectomy to predict the patient's prognosis and guide postoperative review and treatment plans.

The systemic treatment of advanced UCEC is usually chemotherapy and targeted therapy, but the outcome varies from person to person. The mRNA expression profile and the R software package 'pRRophetic' were utilized to predict patients' six drug sensitivities and controls in this investigation. Cisplatin is helpful in individuals with PPAR-related gene somatic mutations, according to our findings. PPAR-related gene CNA patients have high sensitivity to paclitaxel but low sensitivity to docetaxel. These results may help clinicians choose chemotherapeutics for UCEC patients with PPAR-related gene somatic mutations.

In recent years, it has been shown that immune cells and inflammatory factors play a role in the tumor microenvironment. Sufficient activation of effector T cells are a prerequisite for the body to kill tumor cells [25]. The expression of programmed cell death-1 and programmed death ligand-1 are present in up to 80% of EC patients [26]. Immunotherapy has become a promising solution for the treatment of UCEC patients. T cells can recognize neoantigens (nonself-antigens) through HLA molecules on the surface of tumor cells. Many neoantigens provide opportunities for immunotherapy to trigger-specific and effective anticancer immune responses [27]. We found that the total TIL infiltration in the tumor microenvironment of patients with UCEC PPAR-related gene mutations increased, and more neoantigens were produced due to the mutations. It means that patients who have PPAR-related gene mutations may benefit from immunotherapy. It requires more clinical research results of UCEC immunotherapy to confirm, but it is also a good start.

The copy number alternation and mutation of genes ultimately influence cell biological functions by differentially changed RNA transcription and protein translation. In view of the great changes in the PPAR-related gene at the genome level, we further analyzed the RNA transcription and protein translation levels of the PPAR-related gene. Unsurprisingly, the RNA and protein expression levels of PPAR-related gene in UCEC are very different from normal endometrium. In some genes, we have observed consistent changes on these three levels, but in other genes, the changes are not one-to-one correspondence.

Because the expression of RNA can easily be measured from the patient's intraoperative pathological tissue, the RNA expression levels of certain genes in tumor section are new tools for predicting postoperative survival. PPAR-related gene expression varies greatly in different patients. We discovered that the PPAR-related gene panel is closely related to patients' postoperative survival time and can be used to predict patient prognosis. We discovered that CYP21A1, DBI, CPT1A, and ME1 are strongly connected to the prognosis of UCEC patients among the 50 PPAR-associated genes. Among them, CYP21A1 has a hazard ratio of less than one, implying that individuals who overexpress CYP21A1 live longer. The other three genes with hazard ratios greater than one, on the other hand, have the reverse implication. *PPAR risk score*, a prognostic prediction tool, was also developed. The *PPAR risk score* is a strong independent risk factor for the overall survival rate of UCEC patients, according to univariate and multivariate Cox regression analysis. We also developed a nomogram with *PPAR risk score* and clinical factors to make the findings of this study more practical in the clinic (Figure 8). The nomogram is a widely used method for predicting cancer prognosis. It combines the parameters of patients to predict their prognosis using statistical approaches. The accuracy of a nomogram is higher than that of a simple clinical profile of patients due to a combination of factors [18, 28]. The nomogram had better prediction accuracy and could benefit more patients, according to the calibration and decision curve analyses.

This research still has certain limitations. First, the study's initial data comes from cohort sequencing, and the findings must be confirmed by larger cohorts and molecular investigations. Second, in order to determine the appropriate cut-off value, the gene expression data used in this study must be revised. Third, because this is a retrospective study, the patient sample is heterogeneous, which could skew the findings. To confirm the utility of the *PPAR risk score* and nomogram established in this study, more clinical research is needed. In subsequent research, we will investigate and confirm the relation between the PPAR pathway and UCEC.

## 5. Conclusions

In conclusion, we found that PPAR-related gene somatic mutations often occur in UCEC patients. Patients with PPAR-related gene mutations may benefit from immunotherapy and cisplatin therapy. Furthermore, we found that the mRNA transcription level of PPAR-related gene in UCEC is significantly different from that of adjacent tissues/normal uterus. We constructed a scoring tool called *PPAR risk score* which is a strong independent risk factor for the overall survival rate of UCEC patients.

## Data Availability

The data used to support the findings of this study are available from the corresponding author upon request.

## Conflicts of Interest

The authors declare that they have no conflicts of interest.

## Authors' Contributions

Minghui Tang and Jingyao Wang contributed equally to this work.

## Acknowledgments

This study was supported by the National Science Foundation of China (81302249), the Natural Science Foundation of Guangdong Province (2021A1515010941), the Science and Technology Program of Guangdong (2014A020212609), and the Medical Science and Technology Research Foundation of Guangdong (A2018065 and A2016205).

## Supplementary Materials

*Supplementary 1*. Supplementary Figure S1: prediction of chemotherapy treatment outcomes for patients with different PPAR-related gene statuses. Prediction of the sensitivity of four chemotherapy drugs in PPAR-related gene CNA patients (a) and mutation patients (b).

*Supplementary 2*. Supplementary Figure S2: the protein expression level of each PPAR-related-gene between UCEC para-tumor tissues, endometrioid UCEC and serous UCEC.

*Supplementary 3*. Supplementary Table S1: specific details about the PPAR-related gene investigated in this study.

## References

[1] R. L. Siegel, K. D. Miller, and A. Jemal, "Cancer statistics, 2020," *CA: a Cancer Journal for Clinicians*, vol. 70, no. 1, pp. 7–30, 2020.

[2] H. C. Kitchener and E. L. Trimble, "Endometrial cancer state of the science meeting," *International Journal of Gynecological Cancer*, vol. 19, no. 1, pp. 134–140, 2009.

[3] R. Brunmeir and F. Xu, "Functional regulation of PPARs through post-translational modifications," *International Journal of Molecular Sciences*, vol. 19, no. 6, p. 1738, 2018.

[4] L. Peng, H. Yang, Y. Ye et al., "Role of peroxisome proliferator-activated receptors (PPARs) in trophoblast functions," *International Journal of Molecular Sciences*, vol. 22, no. 1, p. 433, 2021.

[5] Y. Wu and S. W. Guo, "Peroxisome proliferator-activated receptor-gamma and retinoid X receptor agonists synergistically suppress proliferation of immortalized endometrial stromal cells," *Fertility and Sterility*, vol. 91, no. 5, pp. 2142–2147, 2009.

[6] K. Ota, K. Ito, T. Suzuki et al., "Peroxisome proliferator-activated receptor gamma and growth inhibition by its ligands in uterine endometrial carcinoma," *Clinical Cancer Research*, vol. 12, no. 14, pp. 4200–4208, 2006.

[7] M. Huang, L. Chen, X. Mao, G. Liu, Y. Gao, X. You et al., "ERR$\alpha$ inhibitor acts as a potential agonist of PPAR$\gamma$ to induce cell apoptosis and inhibit cell proliferation in endometrial cancer," *Aging (Albany NY)*, vol. 12, no. 22, pp. 23029–23046, 2020.

[8] A. Subramanian, P. Tamayo, V. K. Mootha et al., "Gene set enrichment analysis: a knowledge-based approach for interpreting genome-wide expression profiles," *Proceedings of the National Academy of Sciences of the United States of America*, vol. 102, no. 43, pp. 15545–15550, 2005.

[9] F. Sanchez-Vega, M. Mina, J. Armenia et al., "Oncogenic signaling pathways in the cancer genome atlas," *Cell*, vol. 173, no. 2, pp. 321–337.e10, 2018.

[10] E. Cerami, J. Gao, U. Dogrusoz et al., "The cBio cancer genomics portal: an open platform for exploring multidimensional cancer genomics data," *Cancer Discovery*, vol. 2, no. 5, pp. 401–404, 2012.

[11] A. Colaprico, T. C. Silva, C. Olsen et al., "TCGAbiolinks: an R/Bioconductor package for integrative analysis of TCGA data," *Nucleic Acids Research*, vol. 44, no. 8, article e71, 2016.

[12] J. C. Brunson, "Ggalluvial: layered grammar for alluvial plots," *Journal of Open Source Software.*, vol. 5, no. 49, p. 2017, 2020.

[13] G. Yu, L. G. Wang, Y. Han, and Q. Y. He, "clusterProfiler: an R package for comparing biological themes among gene clusters," *OMICS*, vol. 16, no. 5, pp. 284–287, 2012.

[14] A. M. Newman, C. L. Liu, M. R. Green et al., "Robust enumeration of cell subsets from tissue expression profiles," *Nature Methods*, vol. 12, no. 5, pp. 453–457, 2015.

[15] V. Thorsson, D. L. Gibbs, S. D. Brown et al., "The immune landscape of cancer," *Immunity*, vol. 48, no. 4, pp. 812–830.e14, 2018.

[16] P. Geeleher, N. J. Cox, and R. S. Huang, "Clinical drug response can be predicted using baseline gene expression levels and in vitro drug sensitivity in cell lines," *Genome Biology*, vol. 15, no. 3, p. R47, 2014.

[17] P. J. Heagerty, T. Lumley, and M. S. Pepe, "Time-dependent ROC curves for censored survival data and a diagnostic marker," *Biometrics*, vol. 56, no. 2, pp. 337–344, 2000.

[18] A. Iasonos, D. Schrag, G. V. Raj, and K. S. Panageas, "How to build and interpret a nomogram for cancer prognosis," *Journal of Clinical Oncology*, vol. 26, no. 8, pp. 1364–1370, 2008.

[19] T. Van Nyen, C. P. Moiola, E. Colas, D. Annibali, and F. Amant, "Modeling endometrial cancer: past, present, and future," *International Journal of Molecular Sciences*, vol. 19, no. 8, p. 2348, 2018.

[20] A. Stampoliou, P. Arapantoni-Dadioti, and K. Pavlakis, "Epigenetic mechanisms in endometrial cancer," *Journal of BUON*, vol. 21, no. 2, pp. 301–306, 2016.

[21] E. D. Klootwijk, M. Reichold, A. Helip-Wooley et al., "Mistargeting of peroxisomal EHHADH and inherited renal Fanconi's syndrome," *The New England Journal of Medicine*, vol. 370, no. 2, pp. 129–138, 2014.

[22] S. Okamura, H. Yoshino, K. Kuroshima et al., "EHHADH contributes to cisplatin resistance through regulation by tumor-suppressive microRNAs in bladder cancer," *BMC Cancer*, vol. 21, no. 1, p. 48, 2021.

[23] E. Alspach, D. M. Lussier, and R. D. Schreiber, "Interferon $\gamma$ and its important roles in promoting and inhibiting spontaneous and therapeutic cancer immunity," *Cold Spring Harbor Perspectives in Biology*, vol. 11, no. 3, 2019.

[24] L. Ni and J. Lu, "Interferon gamma in cancer immunotherapy," *Cancer Medicine*, vol. 7, no. 9, pp. 4509–4516, 2018.

[25] P. Danaher, S. Warren, R. Lu et al., "Pan-cancer adaptive immune resistance as defined by the Tumor Inflammation Signature (TIS): results from The Cancer Genome Atlas (TCGA)," *Journal for Immunotherapy of Cancer*, vol. 6, no. 1, p. 63, 2018.

[26] Z. Gatalica, C. Snyder, T. Maney et al., "Programmed cell death 1 (PD-1) and its ligand (PD-L1) in common cancers and their correlation with molecular cancer type," *Cancer Epidemiology, Biomarkers & Prevention*, vol. 23, no. 12, pp. 2965–2970, 2014.

[27] M. Roerden, A. Nelde, and J. S. Walz, "Neoantigens in hematological malignancies-ultimate targets for immunotherapy?," *Frontiers in Immunology*, vol. 10, p. 3004, 2019.

[28] Y. W. Won, J. Joo, T. Yun et al., "A nomogram to predict brain metastasis as the first relapse in curatively resected non-small cell lung cancer patients," *Lung Cancer*, vol. 88, no. 2, pp. 201–207, 2015.

Hindawi
PPAR Research
Volume 2021, Article ID 5525091, 7 pages
https://doi.org/10.1155/2021/5525091

*Research Article*

# Variation of PPARG Expression in Chemotherapy-Sensitive Patients of Hypopharyngeal Squamous Cell Carcinoma

**Meng Lian**,[1] **Yong Tao**,[2] **Jiaming Chen**,[1] **Xixi Shen**,[1] **Lizhen Hou**,[1] **Shaolong Cao**,[3] **and Jugao Fang**[1]

[1]*Department of Otorhinolaryngology Head and Neck Surgery, Beijing Tongren Hospital, Capital Medical University, Beijing 100730, China*
[2]*Department of Pharmacy, Liaocheng Third People's Hospital, Liaocheng, Shandong 252000, China*
[3]*Department of Bioinformatics and Computational Biology, The University of Texas MD Anderson Cancer Center, Houston, TX 77030, USA*

Correspondence should be addressed to Jugao Fang; fangjugao2@ccmu.edu.cn

Received 17 February 2021; Accepted 30 April 2021; Published 18 May 2021

Academic Editor: Sha Liu



Our previous study showed that the upregulation of peroxisome proliferator-activated receptor gamma (PPARG) could promote chemosensitivity of hypopharyngeal squamous cell carcinoma (HSCC) in chemotherapeutic treatments. Here, we acquired two more independent expression data of PPARG to validate the expression levels of PPARG in chemotherapy-sensitive patients (CSP) and its individualized variations compared to chemotherapy-non-sensitive patients (CNSP). Our results showed that overall PPARG expression was mildly downregulated (log fold change = −0.55; $p$ value = 0.42; overexpression in three CSPs and reduced expression in four CSPs), which was not consistent with previous results (log fold change = 0.50; $p = 0.22$; overexpression in nine CSPs and reduced expression in three CSPs). Both studies indicated that PPARG expression variation was significantly associated with the Tumor-Node-Metastasis (TNM) stage ($p = 7.45e-7$ and $6.50e-4$, for the first and second studies, respectively), which was used as one of the predictors of chemosensitivity. The new dataset analysis revealed 51 genes with significant gene expression changes in CSPs (LFC > 1 or <-1; $p$ value < 0.01), and two of them (TMEM45A and RBP1) demonstrated strong coexpression with PPARG (Pearson correlation coefficient > 0.6 or <-0.6). There were 21 significant genes in the data from the first study, with no significant association with PPARG and no overlap with the 51 genes revealed in this study. Our results support the connection between PPARG and chemosensitivity in HSCC tumor cells. However, significant PPARG variation exists in CSPs, which may be influenced by multiple factors, including the TNM stage.

## 1. Introduction

Hypopharyngeal squamous cell carcinoma (HSCC) accounts for about 5% of head and neck tumors and is one of the top human malignancies in Europe and the United States [1]. Each year, HSCC causes about 10 cases per million people in the world, with more than 160,000 new cases and 83,000 deaths [2, 3]. Due to the poor survival rate and the devastating impacts on swallowing and speech, the administration of HSCC remains one of the most challenging topics [4]. Patients with HSCC are usually treated with chemoradiotherapy to preserve the organ and its function [5]. PPARG (peroxisome proliferator-activated receptor gamma) is a protein-coding gene, which has been suggested to improve chemosensitivity in human carcinomas, including HSCC [6–9].

Our previous study showed that elevated PPARG expression could drive multiple molecules to increase the chemosensitivity of multiple squamous carcinoma cells [9]. For example, the activation of PPARG was shown to increase the expression of BMP6, BMP7, and NME1 [10, 11], which was positively related to the chemosensitivity of multiple squamous carcinoma c5ells [12–14]. Moreover, PPARG has been suggested to depress the expression of multiple

chemosensitivity inhibitors, such as TERT, CFTR, and EGR1 [9], which form another type of pathway for the chemosensitivity promotion role of PPARG [15–17].

Our previous study also showed that PPARG could demonstrate increased expression levels in HSCC chemotherapy-sensitive patients (CSP) compared to chemotherapy-non-sensitive patients (CNSP) [9], supporting the role of PPARG in chemosensitivity promotion. However, a significant variance was observed among the individuals within the CSP group, resulting in a mild overall expression change. In this study, we explored the expression changes of PPARG in the CSP group by acquiring further expression data and tested the potential influence of multiple clinical parameters. Our results confirmed the association between PPARG and chemosensitivity in HSCC patients as well as its strong expression variance among individual HSCC subjects, which suggested that PPARG may be among multiple factors that influence the chemotherapy sensitivity of HSCC patients.

## 2. Materials and Methods

*2.1. Patient Recruitment and Specimen Selection.* In our previous study, microarray expression data of 21 HSCC patients were acquired, including 12 CSPs and 9 CNSPs [9]. These patients were undergoing induction chemotherapy for primary HSCC. We submitted our data to Gene Expression Omnibus (GEO; https://www.ncbi.nlm.nih.gov/geo/) with GEO ID GSE85608. Following the same data acquisition workflow, we acquired the expression data of another 11 HSCC patients, which is also available on GEO (GEO ID GSE85607). We provided the clinical features of these HSCC patients in Tables 1 and 2, respectively. For more details of the two datasets, please refer to https://www.ncbi.nlm.nih.gov/geo/query/acc.cgi?acc=GSE85608 and https://www.ncbi.nlm.nih.gov/geo/query/acc.cgi?acc=GSE85607, respectively.

*2.2. PPARG Expression and Potential Influential Factors.* For the two datasets, we renalyzed the expression levels of PPARG at probe ILMN_1800225 (probe sequence: CCTGAGCCACTGCCAACATTTCCCTTCTTCCAGTTGCACTATTCTGAGGG), focusing on its variation and potential influential factors. We first compared the expression levels in the CSP group and CNSP group in terms of log fold change (LFC) using one-way ANOVA. Then, we employed a multiple linear regression (MLR) model to study the potential connection between PPARG levels and multiple clinical parameters, including age, TNM stage, histologic differentiation (HD) degree, and chemotherapy response (CR). For the nonnumeric variables, the original string value was changed to a numeric value by indexing different values. Beta values, 95% confidence intervals of beta values, and parameter significance in terms of $p$ values were reported. All the analyses were performed using MATLAB (version R2017a).

*2.3. Coexpression Analysis.* To explore the coinfluential genes that play roles in the CSPs of HSCC disease, we first identified the genes that demonstrated a significant change in the CSP group compared with the CNSP group (LFC > 1 or <-1 and $p < 0.01$) using one-way ANOVA (function "anaova1" in the statistics toolbox of MATLAB). Then, we calculated the pairwise linear correlation between PPARG expression and that of these significant genes (function "corr" in the statistics toolbox of MATLAB). The RHO (Pearson's correlation coefficient) value was used to evaluate the strength of the coexpression: (1) strong correlation: abs(RHO) $\in [0.6, 1]$; (2) medium correlation: abs(RHO) $\in [0.4, 0.6]$; (3) weak correlation: abs(RHO) $\in [0.2, 0.4]$; and (4) no correlation: abs(RHO) $< 0.2$. Here, abs(RHO) refers to the absolute value of RHO. All analyses have been conducted using MATLAB (version R2020a).

*2.4. Pathway Analysis.* To explore the functionality of the significant genes in the CSP group that also presented coexpression with PPARG (abs(RHO) $\geq 0.2$), we conducted Fisher's exact test-based pathway enrichment analysis (PEA) (https://david.ncifcrf.gov/content.jsp?file=functional_annotation.html#fisher) against Gene Ontology (GO) [18]. In addition, a literature-based network analysis was conducted using Pathway Studio (http://www.pathwaystudio.com) to uncover potential cofunctional genes of PPARG. For the detailed instructions regarding network analysis, please refer to the supporting materials at https://supportcontent.elsevier.com/Support%20Hub/Pathway%20Studio/Network%20Builder%20basic%20_Interactive%20NB%20v114.pdf.

## 3. Results

*3.1. PPARG Expression in the CSP Group.* For the two datasets analyzed, we presented the expression of PPARG for all HSCC patients in Figure 1, including both CSPs and CNSPs. In dataset GSE85608, PPARG presented an overall increased expression in the CSP group compared to the CNSP group (LFC = 0.50; $p = 0.22$; see Figure 1(b)). However, in dataset GSE85607, PPARG presented an overall reduced expression (LFC = −0.55; $p = 0.42$), with more patients presented decreased expression than overexpression (four vs. three; see Figure 1(a)). Moreover, there were also significant variances among the CNSP group (green bars in Figures 1(a) and 1(b)). These results suggested that there were influential factors causing the variation of PPARG expression among HSCC patients, which is worthy of further study.

*3.2. TNM Stage and PPARG.* MLR results by using data from both GSE85607 and GSE85608 showed that the expression levels of PPARG were significantly associated with the TNM stage ($p$ value = $6.37e-4$ and $7.57e-7$ for GSE85607 and GSE85608, respectively), as shown in Figure 2. However, due to the limited sample size, TNM stages were not well matched among samples within the two datasets. More data with a larger sample size is needed to better understand the linkage between TNM stage and PPARG expression levels.

To note, the $p$ values for the beta factor of chemotherapy response (CR) did not reach the significance level ($p$ value = 0.16 and 0.26 for GSE85607 and GSE85608, respectively). This was consistent with the mild overall expression changes of PPARG in the CSP group compared with the CNSP group.

Table 1: Clinical data of HSCC patients for GSE85608.

| Subject ID | Age | TNM stage | Histologic differentiation degree | Chemotherapy response | Gender |
|---|---|---|---|---|---|
| S1 | 69 | T4aN2M0 | Moderately differentiated | PR | Male |
| S2 | 62 | T4aN2M0 | Well differentiated | PR | Male |
| S3 | 69 | T4N1M0 | Poorly differentiated | PR | Male |
| S4 | 49 | T3N2M0 | Moderately differentiated | PR | Male |
| S5 | 60 | T4bN2M0 | Moderately differentiated | PR | Male |
| S6 | 69 | T4aN0M0 | Moderately differentiated | PR | Male |
| S7 | 44 | T2N2M0 | Poorly differentiated | PR | Male |
| S8 | 53 | T4aN0M0 | Well differentiated | PR | Male |
| S9 | 49 | T4aN2M0 | Moderately differentiated | PR | Male |
| S10 | 44 | T4aN2M0 | Poorly differentiated | PR | Male |
| S11 | 60 | T3N1M0 | Moderately differentiated | CR | Male |
| S12 | 48 | T4bN2M0 | Well differentiated | PR | Male |
| N1 | 65 | T4aN2M0 | Well differentiated | SD | Male |
| N2 | 45 | T2N3M0 | Moderately differentiated | PD | Male |
| N3 | 57 | T4bN3M1 | Well differentiated | SD | Male |
| N4 | 69 | T3N2M0 | Well differentiated | SD | Male |
| N5 | 71 | T4aN2M0 | Poorly differentiated | SD | Male |
| N6 | 43 | T4bN2M1 | Poorly differentiated | SD | Male |
| N7 | 69 | T2N1M0 | Well differentiated | SD | Male |
| N8 | 71 | T4aN0M0 | Well differentiated | SD | Male |
| N9 | 43 | T4aN2M0 | Moderately differentiated | SD | Male |

Note: CR (complete response): disappearance; confirmed at 4 weeks; PR (partial response): 50% decrease; confirmed at 4 weeks; SD (stable disease): neither PR nor PD criteria are met; PD (progressive disease): 25% increase; no CR, PR, or SD documented before a progressed disease.

Table 2: Clinical data of HSCC patients for GSE85607.

| Subject ID | Gender | Age | TNM stage | Histologic differentiation degree | Chemotherapy response |
|---|---|---|---|---|---|
| S1 | Female | 71 | T2N0M0 | Poorly differentiated | PR |
| S2 | Male | 68 | T2N0M0 | Well differentiated | PR |
| S3 | Male | 55 | T4aN0M0 | Well differentiated | PR |
| S4 | Male | 68 | T3N0M1 | Moderately differentiated | PR |
| S5 | Male | 58 | T3N0M0 | Well differentiated | PR |
| S6 | Male | 52 | T2N0M0 | Well differentiated | PR |
| S7 | Male | 56 | T2N0M0 | Well differentiated | PR |
| N1 | Male | 58 | T4aN3M0 | Poorly differentiated | SD |
| N2 | Male | 61 | T3N2M0 | Poorly differentiated | SD |
| N3 | Male | 56 | T1N0M0 | Well differentiated | SD |
| N4 | Male | 59 | T3N2M0 | Moderately differentiated | PD |

Note: CR (complete response): disappearance; confirmed at 4 weeks; PR (partial response): 50% decrease; confirmed at 4 weeks; SD (stable disease): neither PR nor PD criteria are met; PD (progressive disease): 25% increase; no CR, PR, or SD documented before a progressed disease.

Moreover, the other two parameters, namely, age and histologic differentiation (HD) degree, were not significant factors influencing PPARG expression levels ($p$ value > 0.42). We presented the detailed results in Supplementary Material PPARG_HSCC_CR➔MLR_GSE85607 and MLR_GSE85608. The Supplementary Material PPARG_HSCC_CR is a multiworksheet Excel file that contains additional results of this study, including the MLR analysis results, ANOVA and correlation analysis results, gene set enrichment analysis results, and references for the network analysis.

*3.3. Significant Genes and Coexpression Analysis.* For dataset GSE85607, 51 significant genes (LFC > 1 or <-1; $p < 0.01$) were identified in the comparison between CSP and CNSP groups. The number of significant genes for dataset GSE85608 was 21. To note, there was no overlap between the two groups of significant genes identified, indicating the different overall genomic variances among the HSCC patients recruited in the two studies. We provided the analysis statistics in Supplementary Material PPARG_HSCC_CR➔Corr_GSE85607 and Corr_GSE85608.

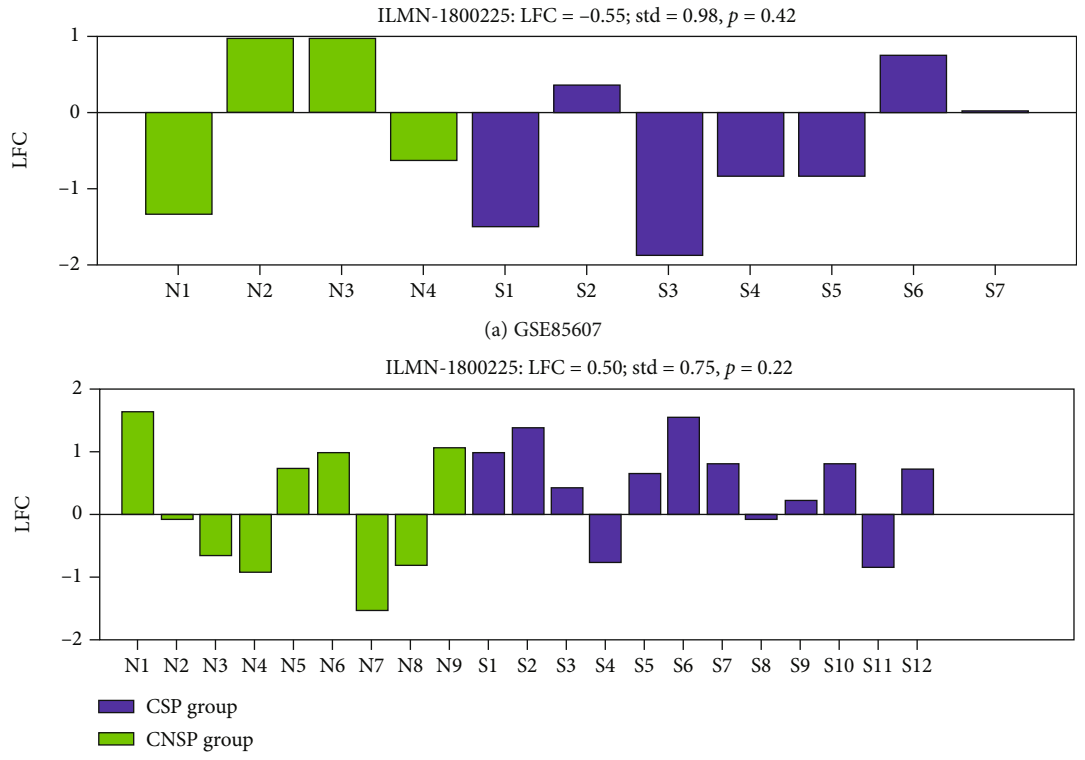


Figure 1: PPARG expression in terms of log fold change (LFC) in chemotherapy-sensitive patients (CSP) among all HSCC patients: (a) PPARG expression of HSCC patients in the dataset GSE85607; (b) PPARG expression of HSCC patients in the dataset GSE85608.

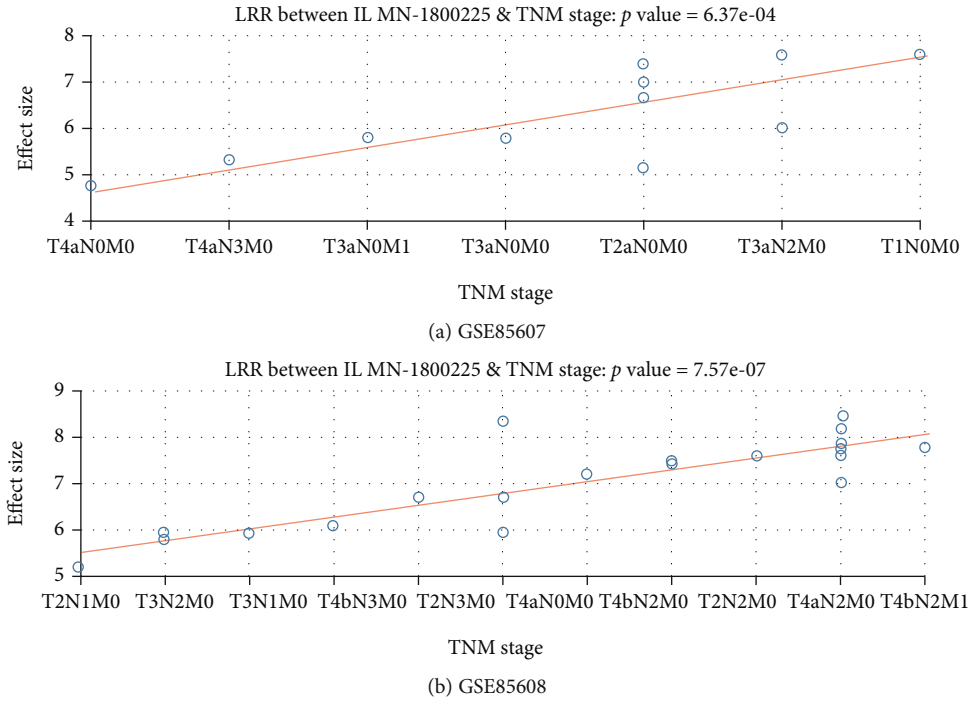


Figure 2: Association between PPARG expression and TNM stage in HSCC patients: (a) association plot by using data of HSCC patients in the dataset GSE85607; (b) association plot by using data of HSCC patients in the dataset GSE85608. The expression levels were log2-transferred.

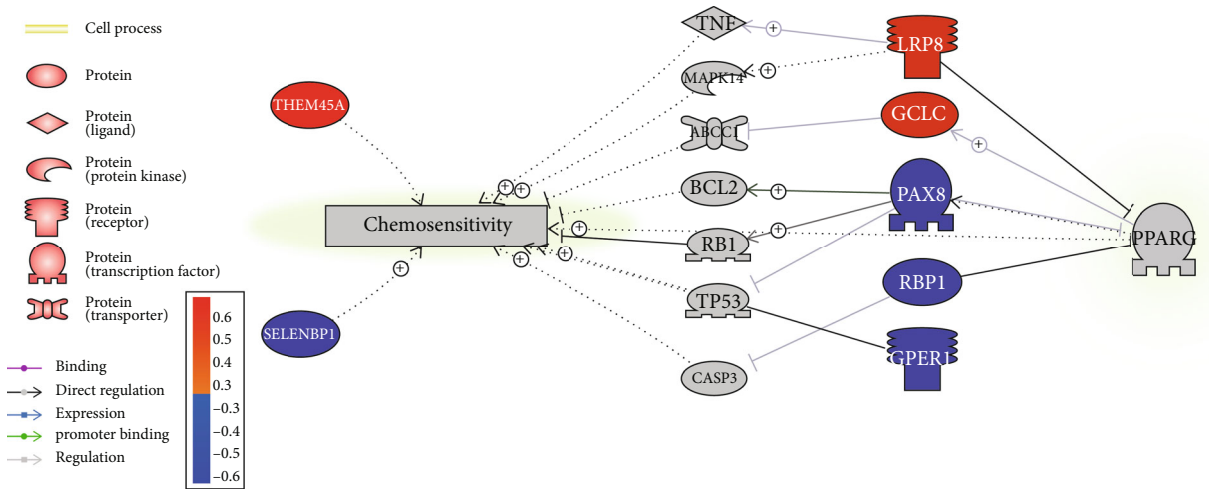


Figure 3: Cofunctional genes of PPARG to play roles in the chemosensitivity in HSCC patients. Nodes in red were positively correlated with PPARG in terms of expression; nodes in blue were negatively correlated with PPARG.

Coexpression analysis showed that, in dataset GSE85607, PPARG was strongly correlated with two genes (RBP1 and TMEM45A) and also presented a weak to moderate correlation with other 19 other genes. Interestingly, PPARG was negatively correlated with the genes that demonstrated overexpression in the CSP group and a positive correlation with downregulated genes. Please see PPARG_HSCC_CR➔Corr_GSE85607 for details. This partially explains the overall downregulation in dataset GSE85607.

In contrast, PPARG was only moderately correlated with one gene (MYOM3; RHO = −0.46) that presented downregulation in the CSP group and weak correlation with seven other genes (see PPARG_HSCC_CR➔Corr_GSE85608). RHO here refers to Pearson's correlation coefficients. Moreover, the genes that showed overexpression were mostly positively correlated with PPARG, while those with reduced expression were all negatively correlated with PPARG. These results partially explain the overall increased PPARG expression in the CSP group of GSE85608.

*3.4. Pathway Enrichment Analysis and Network Analysis.* For the 29 CSP-significant PPARG coexpressed genes from both datasets, we conducted a PEA against the Gene Ontology (GO). However, none of these pathways passed the false discovery rate (FDR) with $q$ value = 0.05. We presented the details in PPARG_HSCC_CR➔PEA. Our results suggested that these genes may not be closely linked to each other in terms of biological functionality.

Literature-based data mining showed that seven out of the 29 CSP-significant genes were linked to PPARG and chemosensitivity, as shown in Figure 3. The network was built based on a total of 334 references, which were provided in PPARG_HSCC_CR➔Ref4Network, including titles and sentences where a relationship has been identified.

It was worthy of mentioning that PPARG presented a positive correlation with two out of three chemosensitivity promoters (LRP8 and GCLC) and a negative correlation with the three chemosensitivity inhibitors (PAX8, GPER, and RBP1), which supports the chemosensitivity promotion role of PPARG in HSCC patients that was proposed in our previous studies.

## 4. Discussion

Our previous study suggested the chemosensitivity promotion role of PPARG in HSCC patients and also indicated the variation of PPARG expression levels among individual HSCC subjects. In this study, we confirmed our previous findings by using two independent expression data of HSCC chemotherapy-sensitive and nonsensitive patients and tested multiple potential influential factors for PPARG expression. Our results suggested that the expression of PPARG was strongly influenced by TNM stage and was correlated with multiple genes that show significant differential expression in CSP/CNSP comparison.

The expression of PPARG was not consistent in the two datasets. Specifically, most CSPs (9 out of 12) in GSE85608 showed overexpression, resulting in overall increased PPARG expression levels in the CSP group. However, in GSE85607, more CSPs (4 out of 7) presented decreased expression, leading to reduced expression levels of PPARG, as shown in Figure 1. These results suggested the variation of PPARG expression in HSCC patients that is worthy of further study.

MLR results showed that PPARG expression in HSCC patients was significantly linked to the TNM stage (Figure 2), which has been implicated as one of the clinical features to predict chemosensitivity [19]. However, due to the limited sample size, the TNM stage was not well matched within the two datasets, which made it difficult to explain the influence of different TNM stages on PPARG expression. Specifically, the highest PPARG expression level was identified in an HSCC patient in the stage of T1N0M0 (Figure 2(a)), which represented a stage that the tumor development was at its earliest stage, with no significant influence on the regional lymph nodes and no metastasis. The lowest PPARG expression was observed from an HSCC patient in a stage of T4aN0M0, which means that the tumor size and

extension of the primary tumor were at the late stage, but with no influence on regional lymph nodes and no metastasis. In contrast, for dataset GSE85608, the highest PPARG expression was observed in an HSCC patient at the stage of T4aN2M1, which means that the development of the tumor in this patient was at its late stage with moderate influence on the regional lymph nodes and early appearance of metastasis. Studies with a larger sample size covering all different TNM stages should be conducted to fully understand the correlation between PPARG expression in HSCC patients and their TNM stages.

Consistent with the mild expression changes of PPARG in the CSP group compared with the CNSP group, chemotherapy response (CR) was moderately correlated with the expression of PPARG ($p$ value = 0.16 and 0.26 for GSE85607 and GSE85608, respectively). Moreover, age and histologic differentiation (HD) degree were shown to be nonsignificant factors for PPARG expression levels ($p$ value > 0.42). Please refer to PPARG_HSCC_CR➔MLR_GSE85607 and MLR_GSE85608 for more details of the MLR results.

The significant variation of PPARG in HSCC CSPs suggested that there were other factors cofunctioning with PPARG to influence the chemosensitivity of HSCC patients. However, among the genes that showed significant expression variance in CSP/SNSP comparison, only a small portion (9 out of 72 genes) showed a moderate to strong correlation with that of PPARG (absolute value of RHO > 0.4). Please refer to PPARG_HSCC_CR➔Corr_GSE85607 and Corr_GSE85608 for the details of coexpression analysis. Among these genes, 7 genes were implicated to have a relation with PPARG and chemosensitivity, as shown in Figure 3. These genes could be the cofunctional factors that work with PPARG to influence the chemosensitivity of HSCC patients. For instance, LRP8 was shown to activate TNF and MARK14 [20, 21], which are promoters of chemosensitivity [22, 23]. In addition, overexpression of GCLC mRNA suppresses the expression of MRP1 [24], which in turn could improve the chemosensitivity in lung cancer patients [25]. The positive correlation between PPARG and LRP8 and GCLC indicated the cofunctionality of these genes and PPARG in the chemosensitivity promotion of HSCC patients. On the other hand, PPARG was negatively correlated with multiple inhibitors of chemosensitivity, including PAX8, GPER1, and RBP1. Yu et al. showed that the blockage of GPER/ABCG2 signaling could be a potential target for enhancing the chemosensitivity of breast cancer patients [26]. Chen et al. showed that RBP1 gene transfection could significantly reverse L5-induced increases in CASP3 [27], while overexpression of CASP3 has been shown to enhance chemosensitivity in multiple cancer cells, including breast cancer cells and hematological neoplastic cells [28, 29]. This establishes a chemosensitivity inhibition role of RBP1. Therefore, the negative correlation between PPARG and RBP1 supports the enhancement effect of PPARG on chemosensitivity.

However, we also noticed that PPARG presented a weak negative correlation with SELENBP1 (RHO = −0.24), which has been shown to increase the chemosensitivity of gastric cancer cells [30]. This may add to the explanation of the variation of PPARG in the CSP group of HSCC patients.

This study has several limitations that need further work. First, although we employed two independent datasets, both of them had small sample sizes. More studies with a larger sample size should be conducted to validate the findings of this study. Second, the identified coexpression factors of PPARG lack replication in other studies regarding their relation to chemosensitivity, which needs further validation.

## 5. Conclusion

Our results support the previous finding that PPARG expression was linked to chemosensitivity in HSCC patients. However, both increased and reduced PPARG expression could happen in chemotherapy-sensitive patients, which may be influenced by factors including the TNM stage.

## Data Availability

The data in our study are available from the corresponding author upon reasonable request.

## Conflicts of Interest

The authors declare that there is no conflict of interest regarding the publication of this paper.

## Acknowledgments

This work was partially supported by the Beijing Administration of Traditional Chinese Medicine (QN2018-32); Beijing Municipal Administration of Hospitals' Ascent Plan (DFL20180202); the Priming Scientific Research Foundation for the Junior Researcher in Beijing Tongren Hospital, Capital Medical University (2018-YJJ-ZZL-006); the Beijing Natural Science Foundation Program and Scientific Research Key Program of Beijing Municipal Commission of Education (KZ201910025034); the Capital Health Research and Development of Special (No. 2018-2-2054); and the Liaoning Natural Science Foundation Program (No. 2019-ZD-0901).

## References

[1] G. Marioni, "Letter to the editors: essentials for an updated epidemiology of laryngeal carcinoma," *Cancer Treatment Reviews*, vol. 38, no. 6, p. 559, 2012.

[2] K. D. Miller, A. Goding Sauer, A. P. Ortiz et al., "Cancer statistics for Hispanics/Latinos, 2018," *CA: a Cancer Journal for Clinicians*, vol. 68, no. 6, pp. 425–445, 2018.

[3] J. Zhou, Z. Ke, L. Ma, M. Liu, and W. Zhang, "Downregulation of miR-204 is associated with poor prognosis and promotes cell proliferation in hypopharyngeal squamous cell carcinoma (HSCC)," *International Journal of Clinical and Experimental Pathology*, vol. 10, no. 7, pp. 7968–7974, 2017.

[4] G. Omura, M. Ando, Y. Ebihara et al., "The prognostic value of TP53 mutations in hypopharyngeal squamous cell carcinoma," *BMC Cancer*, vol. 17, no. 1, p. 898, 2017.

[5] X. Liu, W. Zhao, and X. Wang, "Inhibition of long non-coding RNA MALAT1 elevates microRNA-429 to suppress the

progression of hypopharyngeal squamous cell carcinoma by reducing ZEB1," *Life Sciences*, vol. 262, article 118480, 2020.

[6] L. Zhan, H. Zhang, Q. Zhang et al., "Regulatory role of KEAP1 and NRF2 in PPAR$\gamma$ expression and chemoresistance in human non-small-cell lung carcinoma cells," *Free Radical Biology & Medicine*, vol. 53, no. 4, pp. 758–768, 2012.

[7] A. P. Kumar, S. Y. Loo, S. W. Shin et al., "Manganese superoxide dismutase is a promising target for enhancing chemosensitivity of basal-like breast carcinoma," *Antioxidants & Redox Signaling*, vol. 20, no. 15, pp. 2326–2346, 2014.

[8] Y. Zhang, H. Y. Luo, G. L. Liu et al., "Prognostic significance and therapeutic implications of peroxisome proliferator-activated receptor $\gamma$ overexpression in human pancreatic carcinoma," *International Journal of Oncology*, vol. 46, no. 1, pp. 175–184, 2015.

[9] M. Lian, J. Chen, X. Shen, L. Hou, and J. Fang, "Pparg may promote chemosensitivity of hypopharyngeal squamous cell carcinoma," *PPAR Research*, vol. 2020, Article ID 6452182, 6 pages, 2020.

[10] M. Takeda, F. Otsuka, H. Otani et al., "Effects of peroxisome proliferator-activated receptor activation on gonadotropin transcription and cell mitosis induced by bone morphogenetic proteins in mouse gonadotrope L$\beta$T2 cells," *The Journal of Endocrinology*, vol. 194, no. 1, pp. 87–99, 2007.

[11] C. H. Chuang, C. L. Yeh, S. L. Yeh, E. S. Lin, L. Y. Wang, and Y. H. Wang, "Quercetin metabolites inhibit MMP-2 expression in A549 lung cancer cells by PPAR-$\gamma$ associated mechanisms," *The Journal of Nutritional Biochemistry*, vol. 33, pp. 45–53, 2016.

[12] W. J. Lian, G. Liu, Y. J. Liu, Z. W. Zhao, T. Yi, and H. Y. Zhou, "Downregulation of BMP6 enhances cell proliferation and chemoresistance via activation of the ERK signaling pathway in breast cancer," *Oncology Reports*, vol. 30, no. 1, pp. 193–200, 2013.

[13] L. S. Wang, K. C. Chow, Y. C. Lien, K. T. Kuo, and W. Y. Li, "Prognostic significance of nm23-H1 expression in esophageal squamous cell carcinoma," *European Journal of Cardio-Thoracic Surgery*, vol. 26, no. 2, pp. 419–424, 2004.

[14] X. Q. Yang, Z. M. Zhang, D. Wang, G. Wang, L. L. Zeng, and Z. Z. Yang, "nm23-H1-siRNA enhances the chemosensitivity to liposome-encapsulated paclitaxel in lung adenocarcinoma cells in vitro," *Zhonghua Zhong Liu Za Zhi*, vol. 33, no. 6, pp. 405–409, 2011.

[15] X. Guo, W. Wang, F. Zhou et al., "siRNA-mediated inhibition of hTERT enhances chemosensitivity of hepatocellular carcinoma," *Cancer Biology & Therapy*, vol. 7, no. 10, pp. 1555–1560, 2008.

[16] J. Zhou, W. Dai, and J. Song, "miR-1182 inhibits growth and mediates the chemosensitivity of bladder cancer by targeting hTERT," *Biochemical and Biophysical Research Communications*, vol. 470, no. 2, pp. 445–452, 2016.

[17] T. Zhao, F. Hu, X. Liu, and Q. Tao, "Blockade of telomerase reverse transcriptase enhances chemosensitivity in head and neck cancers through inhibition of AKT/ERK signaling pathways," *Oncotarget*, vol. 6, no. 34, pp. 35908–35921, 2015.

[18] A. Subramanian, P. Tamayo, V. K. Mootha et al., "Gene set enrichment analysis: a knowledge-based approach for interpreting genome-wide expression profiles," *Proceedings of the National Academy of Sciences of the United States of America*, vol. 102, no. 43, pp. 15545–15550, 2005.

[19] D. He, D. Ma, and E. Jin, "Dynamic breast magnetic resonance imaging: pretreatment prediction of tumor response to neoadjuvant chemotherapy," *Clinical Breast Cancer*, vol. 12, no. 2, pp. 94–101, 2012.

[20] E. M. Gleeson, J. S. O'Donnell, E. Hams et al., "Activated factor X signaling via protease-activated receptor 2 suppresses pro-inflammatory cytokine production from lipopolysaccharide-stimulated myeloid cells," *Haematologica*, vol. 99, no. 1, pp. 185–193, 2014.

[21] D. Baitsch, H. H. Bock, T. Engel et al., "Apolipoprotein E induces antiinflammatory phenotype in macrophages," *Arteriosclerosis, Thrombosis, and Vascular Biology*, vol. 31, no. 5, pp. 1160–1168, 2011.

[22] I. Gkouveris, N. Nikitakis, and A. Sklavounou, "p38 expression and modulation of STAT3 signaling in oral cancer," *Pathology Oncology Research*, vol. 26, no. 1, pp. 183–192, 2020.

[23] X. Lou, Q. Zhou, Y. Yin, C. Zhou, and Y. Shen, "Inhibition of the met receptor tyrosine kinase signaling enhances the chemosensitivity of glioma cell lines to CDDP through activation of p38 MAPK pathway," *Molecular Cancer Therapeutics*, vol. 8, no. 5, pp. 1126–1136, 2009.

[24] Y. Yamane, M. Furuichi, R. Song et al., "Expression of multidrug resistance protein/GS-X pump and $\gamma$-glutamylcysteine synthetase genes is regulated by oxidative stress∗," *The Journal of Biological Chemistry*, vol. 273, no. 47, pp. 31075–31085, 1998.

[25] N. Bandi and U. B. Kompella, "Budesonide reduces multidrug resistance-associated protein 1 expression in an airway epithelial cell line (Calu-1)," *European Journal of Pharmacology*, vol. 437, no. 1-2, pp. 9–17, 2002.

[26] T. Yu, H. Cheng, Z. Ding et al., "GPER mediates decreased chemosensitivity via regulation of ABCG2 expression and localization in tamoxifen-resistant breast cancer cells," *Molecular and Cellular Endocrinology*, vol. 506, article 110762, 2020.

[27] C. Chen, L. Ke, H. Chan et al., "Electronegative low density lipoprotein induces renal apoptosis and fibrosis: STRA6 signaling involved," *Journal of Lipid Research*, vol. 57, no. 8, pp. 1435–1446, 2016.

[28] L. Y. Bourguignon, W. Xia, and G. Wong, "Hyaluronan-mediated CD44 interaction with p300 and SIRT1 regulates $\beta$-catenin signaling and NF$\kappa$B-specific transcription activity leading to MDR1 and Bcl-$x_L$ gene expression and chemoresistance in breast tumor cells∗," *The Journal of Biological Chemistry*, vol. 284, no. 5, pp. 2657–2671, 2009.

[29] I. M. Santos-Pirath, L. O. Walter, M. F. Maioral et al., "Apoptotic events induced by a natural plastoquinone from the marine alga *Desmarestia menziesii* in lymphoid neoplasms," *Experimental Hematology*, vol. 86, pp. 67–77.e2, 2020.

[30] C. Zhang, W. Xu, W. Pan et al., "Selenium-binding protein 1 may decrease gastric cellular proliferation and migration," *International Journal of Oncology*, vol. 42, no. 5, pp. 1620–1629, 2013.

Hindawi
PPAR Research
Volume 2021, Article ID 5518138, 8 pages
https://doi.org/10.1155/2021/5518138

*Research Article*

# PPARD May Play a Protective Role for Major Depressive Disorder

**Tao Yang**[1], **Juhua Li**[1], **Liyuan Li**[1], **Xuehua Huang**[1], **Jiajun Xu**[1], **Xia Huang**[1], **Lijuan Huang**[1] and **Kamil Can Kural**[2]

[1]*Mental Health Center, West China Hospital, Sichuan University, Chengdu, China*
[2]*School of Systems Biology, George Mason University, Manassas, VA 20110, USA*

Correspondence should be addressed to Xuehua Huang; huangxuehua10@gousinfo.com

Received 23 January 2021; Revised 28 March 2021; Accepted 8 April 2021; Published 21 April 2021

Academic Editor: Anastasia Nesterova



Activation of PPARD has been shown to inhibit depressive behaviors and enhances neurogenesis. However, whether PPARD is involved in the pathological development of major depressive disorder (MDD) is largely unknown. To explore the potential connection between PPARD and MDD, we first conducted a literature-based data mining to construct a PPARD-driven MDD regulating network. Then, we tested the PPARD expression changes in MDD patients from 18 independent MDD RNA expression datasets, followed by coexpression analysis, multiple linear regression analysis, and a heterogeneity analysis to study the influential factors for PPARD expression levels. Our results showed that overexpression of PPARD could inhibit inflammatory cytokine signaling pathways and the ROS and glutamate pathways that have been shown to play important roles in the pathological development of MDD. However, PPARD could also activate nitric oxide formation and ceramide synthesis, which was implicated as promoters in the pathogenesis of MDD, indicating the complexity of the relationship between PPARD and MDD. PPARG presented significant within- and between-study variations in the 18 MDD datasets ($p$ value = 0.97), which were significantly associated with the population region (country) and sample source ($p < 2.67e-5$). Our results suggested that PPARD could be a potential regulator rather than a biomarker in the pathological development of MDD. This study may add new insights into the understanding of the PPARD-MDD relationship.

## 1. Introduction

Major depressive disorder (MDD), also known as depression, is a mental disorder characterized by at least two weeks of pervasive low mood. The leading cause of MDD is believed to be a combination of genetic and environmental factors [1–7], with about 40% of the risk related to genetics [4].

Peroxisome proliferator-activated receptor beta/delta (PPARD) is one of the three known PPARs (the others are PPAR$\alpha$ and PPAR$\gamma$), which are part of the nuclear receptor superfamily of transcription factors. PPARD governs diverse biological processes [8] and shows a widespread brain expression, with particularly high levels in the hippocampus, entorhinal cortex, and hypothalamus [9, 10].

Several previous studies show that PPARD might be involved in depression occurrences [11, 12]. Specifically, the hippocampal genetic knockdown of PPARD has been shown to cause depression-like behaviors and neurogenesis suppression [12], suggesting that PPARD plays a crucial role in neurogenesis and regulates both depression and memory. Moreover, hippocampal PPARD overexpression or activation inhibits stress-induced depressive behaviors and enhances neurogenesis [11]. However, so far, whether PPARD is involved in MDD and its related underlying mechanism is largely unknown.

Here, we hypothesized that PPARD could play a role in the pathological development of MDD. Our results supported this hypothesis and indicated that deficiency of PPARD might be involved in the pathogenesis of MDD by regulating cytokine-related signaling pathways. However, our results also demonstrate the variation of PPARD expressions in the cases of MDD, which may be influenced by multiple factors, including sample postulation regions. Our study might add new insights into the understanding of the roles that PPARD plays in MDD.

## 2. Method

The rest of this study is organized as follows. First, we conducted a systematic literature-based network analysis to

explore the possible relationship between PPARD and MDD. Then, we analyzed the expression of PPARD in 18 public human RNA array-expression datasets linked with MDD diagnosis. After that, we employed multiple linear regression analysis to study the potential, influential factors of PPARD expression in the cases of MDD. To facilitate the understanding of the results presented, we provided additional supporting data and information in a supplementary material named PPARD_MDD.

*2.1. Literature-Based Pathway Analysis.* Assisted by Pathway Studio (PS) (http://www.pathwaystudio.com; version 12.3.0.16), we conducted a systematical pathway analysis to uncover PPARD-driven MDD regulators at different levels, including proteins, small molecules, complexes, and functional classes. Owned by Elsevier Inc., the PS database ResNet [13] contains functional relationships and pathways of mammalian proteins, including human, mouse, and rat genes. The database covers over 24 million PubMed abstracts and 3.5 million Elsevier and 3rd part full-text papers.

The MDD regulators were identified by using the Shortest Path Module within Pathway Studio (https://supportcontent.elsevier.com/Support%20Hub/Pathway%20Studio/Guide%20to%20Building%20Pathways%20in%20Mammal%20with%20Pathway%20Studio%20Web.pdf). Each relation between MDD and its regulators was supported by one or more references, as shown in Ref4Pathway in the Supplementary Materials (available here). The sentences from each supporting reference were manually checked for quality control. Following the same process, the items influenced by PPARD were also identified, with the overlapped items used to build the PPARD-driven MDD regulating network.

The following criteria were applied for the selection of the PPARD-driven MDD regulators. (1) The direction is from PPARD to MDD. (2) Each relationship (network edge) has a signed polarity (positive or negative effect). (3) The quality control of each relationship (network edge) was conducted through manual inspection of the supporting references. (4) The type of regulators includes genes (proteins), functional class, and small molecules. For a relationship with more than 10 supporting references, we inspected the first 10 references. The relationships that passed the filtering criteria were employed to construct the PPARD-driven signaling pathways that may affect roles in the pathology of MDD. We provided the details of these identified relationships and the underlying supporting references in Ref4Pathway in the Supplementary Materials, including the reference title and the sentences where a relationship has been identified.

*2.2. MDD RNA Expression Data Acquisition.* To explore the quantitative change of PPARD in MDD patients and test whether PPARD could work as a biomarker for MDD, we conducted an MDD RNA expression data-based analysis on PPARD expression. We acquired MDD RNA array-expression datasets from GEO (https://www.ncbi.nlm.nih.gov/geo/). Initially, we searched with the keyword "major depressive disorder" and identified 317 studies with series data. Then, the following criteria were applied to fulfill the purpose of this study, including the following:

(1) The data type was RNA expression by array

(2) The organism of datasets was *Homo sapiens*

(3) The study design was MDD vs. healthy control

(4) The total number of samples was not less than 10

(5) The dataset and corresponding format files were feasibly available and downloadable

There were 18 datasets that satisfied the selection criteria and were included for expression analysis. We provided the information employed in this study of these datasets in Table 1, and the GEOID can be used to retrieve the detailed description of each dataset at https://www.ncbi.nlm.nih.gov/geo/.

*2.3. Expression of PPARD in MDD RNA Expression Datasets.* In this study, the expression for PPARD was estimated for each of the 18 datasets listed in Table 1. Specifically, we first calculated the fold change that was defined as the ratio between the mean expression of MDD cases and that of healthy controls. Then, the log2-transferred fold change (LFC) was used as effect size, such that fold changes lower than one become negative, while those greater than one become positive. The significance criteria were set as abs $(\mathrm{LFC}) \geq 1$ and $p < 0.05$.

*2.4. Coexpression Analysis.* Using the 18 MDD RNA expression datasets, we also studied the coexpression between PPARD and its driven genes regulating MDD. The purpose of the coexpression analysis was to validate the relationships between PPARD and its driven genes at the gene expression level. In the datasets where PPARD showed a small effect size ($\mathrm{LFC} \in [-0.3, 0.3]$), we assumed that PPARD exerted no influence on its driven genes. Thus, the analysis only focused on PPARD with significant changes.

*2.5. Heterogeneity Analysis of PPARD Expression.* A heterogeneity analysis was conducted to study the variance within and between different studies [14] to determine if there was a significant between-study variance compared with within-study variance. The analysis was conducted by using MATLAB (R2017a) with the results presented in ExpressionOfPPARD in the Supplementary Materials.

*2.6. Multiple Linear Regression Analysis.* To investigate the possible influential factors for the gene expression of PPARD in the case of MDD, we conducted a multiple linear regression (MLR) analysis on five parameters, including sample size, sample population region (country), sample source, data acquisition platform, and study age. $p$ value $< 0.05$ was set as a significance criterion for the identification of significant factors. The analysis was performed using the statistic toolbox "regress()" in MATLAB (R2017a).

Table 1: The 18 major depression disorder RNA expression datasets from GEO.

| Dataset GEOID | Data contributors | # control/cases | Country | Study age | Platform | Sample source | Sample organism |
|---|---|---|---|---|---|---|---|
| GSE12654 | Iwamoto et al., 2008 | 15/11 | Japan | 13 | GPL8300 | Brodmann area | *Homo sapiens* |
| GSE32280 | Yi et al., 2012 | 8/16 | China | 9 | GPL570 | Blood | *Homo sapiens* |
| GSE44593 | Sibille et al., 2016 | 14/14 | USA | 5 | GPL570 | Amygdala | *Homo sapiens* |
| GSE53987 | Lanz et al., 2014 | 18/16 | USA | 7 | GPL570 | Multiple brain region | *Homo sapiens* |
| GSE54562 | Sibille et al., 2014 | 10/10 | USA | 7 | GPL6947 | Anterior cingulate cortex | *Homo sapiens* |
| GSE54563 | Sibille et al., 2014 | 25/25 | USA | 7 | GPL6947 | Anterior cingulate cortex | *Homo sapiens* |
| GSE54564 | Sibille et al., 2014 | 21/21 | USA | 7 | GPL6947 | Amygdala | *Homo sapiens* |
| GSE54565 | Sibille et al., 2014 | 16/16 | USA | 7 | GPL570 | Anterior cingulate cortex | *Homo sapiens* |
| GSE54566 | Sibille et al., 2014 | 14/14 | USA | 7 | GPL570 | Amygdala | *Homo sapiens* |
| GSE54567 | Sibille et al., 2014 | 14/14 | USA | 7 | GPL570 | Dorsolateral prefrontal cortex | *Homo sapiens* |
| GSE54568 | Sibille et al., 2014 | 15/15 | USA | 7 | GPL570 | Dorsolateral prefrontal cortex | *Homo sapiens* |
| GSE54570 | Sibille et al., 2014 | 13/13 | USA | 7 | GPL96 | Dorsolateral prefrontal cortex | *Homo sapiens* |
| GSE54571 | Sibille et al., 2014 | 13/13 | USA | 7 | GPL570 | Anterior cingulate cortex | *Homo sapiens* |
| GSE54572 | Sibille et al., 2014 | 12/12 | USA | 7 | GPL570 | Anterior cingulate cortex | *Homo sapiens* |
| GSE54575 | Sibille et al., 2014 | 12/12 | USA | 7 | GPL96 | Orbital ventral prefrontal cortex | *Homo sapiens* |
| GSE92538 | Hagenauer et al., 2016 | 56/29 | USA | 5 | GPL10526 | DLPFC | *Homo sapiens* |
| GSE98793 | Kelly et al., 2017 | 64/128 | UK | 4 | GPL570 | Blood | *Homo sapiens* |
| GSE114852 | Breen et al., 2018 | 85/31 | USA | 3 | GPL10558 | Blood | *Homo sapiens* |

Note: "study age" of a dataset was defined as the current year—the year of data submission.

## 3. Results

*3.1. PPARD-Driven Network.* Literature-based network analysis revealed nine entities regulated by PPARD that were also upstream regulators of MDD, as shown in Figure 1. Among these entities, increased PPARD could exert a major positive influence on MDD by upregulation of one MDD inhibitors (tetrahydrobiopterin) and downregulation of 6 MDD promoters, including two cytokine genes (IL6 and TNF), two small molecules (ROS and glutamate), and the two functional classes (cytokine and inflammatory cytokine). These MDD regulators were highlighted in green in Figure 1. However, PPARD may also activate nitric oxide production (NO) and ceramide, two promoters of MDD (highlighted in red in Figure 1). Overall, these literature data mining-based relationships suggested that the deficiency of PPARD might facilitate the development of MDD by activating cytokine classes and promoting the secretion of reactive oxygen species (ROS) and glutamate. The pathways presented in Figure 1 were based on over 300 independent studies. The reference information was provided in Ref4Pathway in the Supplementary Materials. To note, over 400 references were listed as some references support multiple relationships.

Specifically, there were about 250 studies (references) supporting the PPARD → cytokine genes → MDD pathways. In vitro cell line expression studies of both human and animal models showed that PPARD reduces the expression and secretion of cytokines, including inflammatory cytokines and pro-inflammatory cytokines. While clinical studies and animal models showed that cytokines could induce sickness behavior with depression-like symptoms, contribute to cognitive decline, and induce MDD. Therefore, inhibition of cytokines by PPARD supports the suppression role of PPARD in the pathological development of MDD.

Moreover, there were 54 references that support the PPARD → ROS → MDD pathway. In vitro human cell line studies showed that activation of PPARD reduces radiation and angiotensin II-induced ROS generation by modulating the expression of SIRT1. And ROS have been suggested to play an important role in the pathogenesis of MDD in clinical studies and animal models.

In addition, 94 references support the PPARD → glutamate → MDD pathway. Both in vitro and human studies show that heightened glutamate plays an important role in the pathophysiology of MDD. In vitro cell line and animal studies showed that activation of PPARD inhibits glutamate release.

There were also two studies that suggested a PPARD → -tetrahydrobiopterin → MDD pathway. Tetrahydrobiopterin has been reported to improve clinical depression by increasing TH activity. Activation of PPARD enhances the regenerative capacity of human endothelial progenitor cells by stimulating the biosynthesis of tetrahydrobiopterin.

On the other hand, there were 22 studies (references) that support the PPARD → NO → MDD relationship, and nine studies (references) support the PPARD → ceramide → MDD relationship. These studies suggested that increased PPARD could increase the production of NO and ceramide in the plasma of the human body. In clinical studies and animal model studies, increased production of NO and ceramide has been

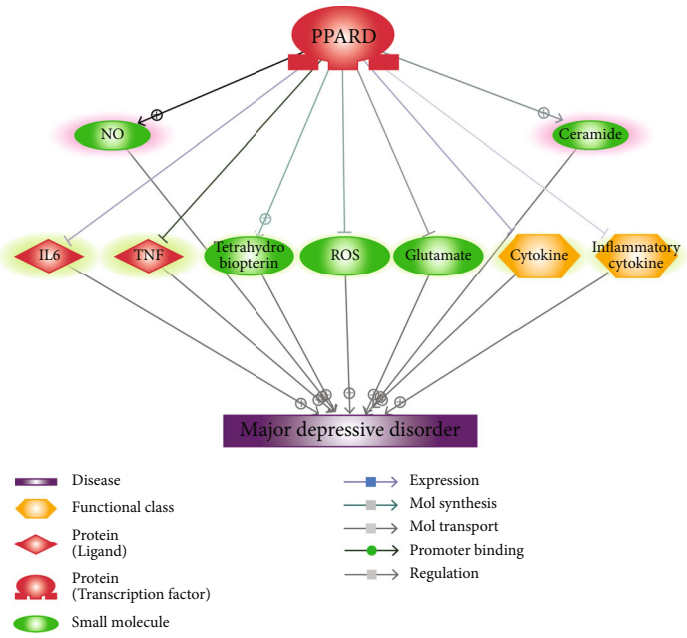


Figure 1: PPARD-driven pathways involved in the pathology of MDD. The pathway was built through Pathway Studio-assisted literature data mining, supported by over 400 references. The items highlighted in green are the ones that were driven by PPARD to suppress the development of MDD, and the red ones were regulated by PPARD to promote MDD development.

shown to promote the development of neuroinflammation-associated disorders, including MDD. Therefore, increased PPARD may have the promotion effect on MDD through the activation of NO and ceramide.

*3.2. Expression Variation of PPARD in 18 MDD Expression Datasets.* To explore the expression changes of PPARD in the cases of MDD, we calculated the LFC of PPARD in the MDD patients compared to healthy controls using 18 different RNA expression datasets, as shown in Figure 2(a). The expression of PPARD demonstrated varies among different studies, ranging from -0.38 to 0.61 ($\text{LFC} = 0.013 \pm 0.19$). Among these datasets, seven presented mild decreased expression ($\text{LFC} = -0.13 \pm 0.11$). The majority of datasets (10 out of 18) showed increased expression of PPARD in MDD patients compared to healthy controls ($\text{LFC} = 0.13 \pm 0.17$). However, none of these changes was identified as significant. The datasets were collected from four different countries, eight different sample sources, and six different platforms, which may well represent different cases of MDD. Our results suggested that PPARD might not present significant changes among MDD patients. For more details of the PPAR expression data analysis, please refer to ExpressionOfPPARD in the Supplementary Materials.

*3.3. Coexpression Analysis.* For the datasets that showed the lowest PPARD expression levels (GSE32280: $\text{LFC} = -0.38$) and highest expression levels (GSE12654: $\text{LFC} = 0.60$), PPARD demonstrated a significant negative correlation with IL6 (Fisher $Z$ transferred Pearson $r = -0.41$; $p = 0.030$) and TNF (Fisher $Z$ transferred Pearson $r = -0.38$; $p = 0.035$). These results indicated that when PPARD expression got activated, TNF expression was inhibited, helping the suppression of MDD. On the other hand, when PPARD was downregulated, IL6 presented overexpression, promoting the development of MDD. We assumed that, when PPARD showed small expression changes ($\text{LFC} \in (-0.3, 0.3)$), it had limited influence on either TNF or IL6. Thus, coexpression analysis was not effective in evaluating the relation between PPARD and these two genes. We provided the results in ExpressionOfPPARD in the Supplementary Materials. Our results support the PPARD → TNF and PPARD ➔ IL6 regulation identified in Figure 1.

*3.4. Multiple Linear Regression Analysis Results.* MLR results showed that out of the five factors tested, only the population region (country) and sample source were significant influential factors ($p = 4.47E-07$ and $2.67E-05$, respectively) for PPARD expression in MDD patients, as shown in Figure 3. However, the other three factors, namely, sample size, study age, and platform, were not significant factors for the expression of PPARD in the case of MDD ($p > 0.15$). For the details of MLR results, please refer to MLR_Results in the Supplementary Materials.

*3.5. Heterogeneity Analysis.* The heterogeneity analysis was employed to test whether the total variance mainly resulted from between-study variance or from both within- and between-study variance. The analysis results showed that the total variance among different studies was 7.9, which was smaller than the expected variance (17) given that all studies have the same actual effect. Our results indicated that the between-study variance was not the primary source contributing to total variance among these studies ($p$ value = 0.96). In other words, there were significant within-study variances among these datasets, as shown in Figure 4. To note, the

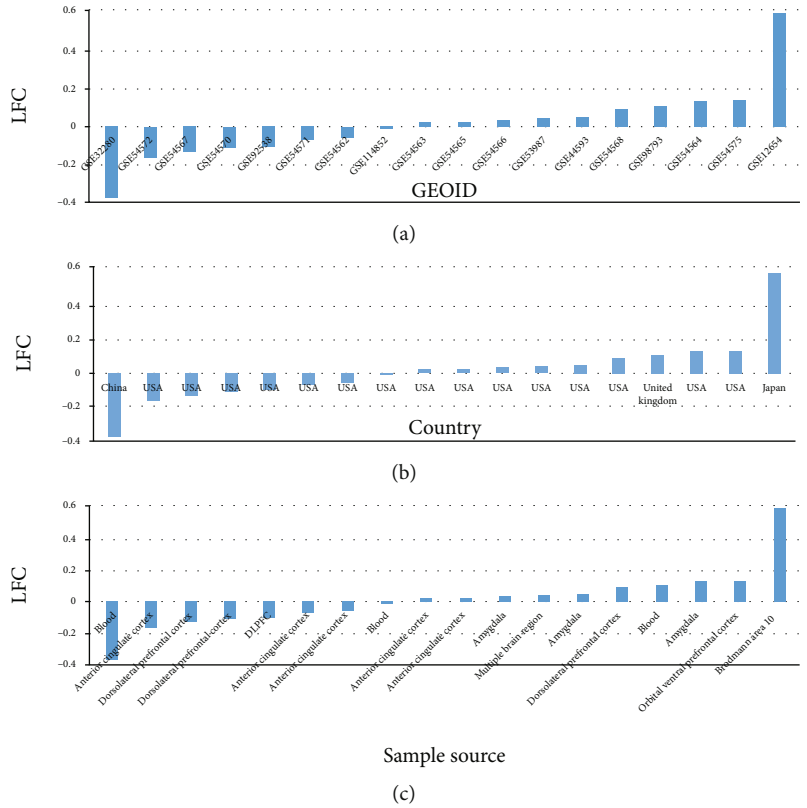


Figure 2: Expression of PPARD in 18 MDD RNA expression datasets: (a) the expression by datasets; (b) the expression by country; (c) the expression by sample source.

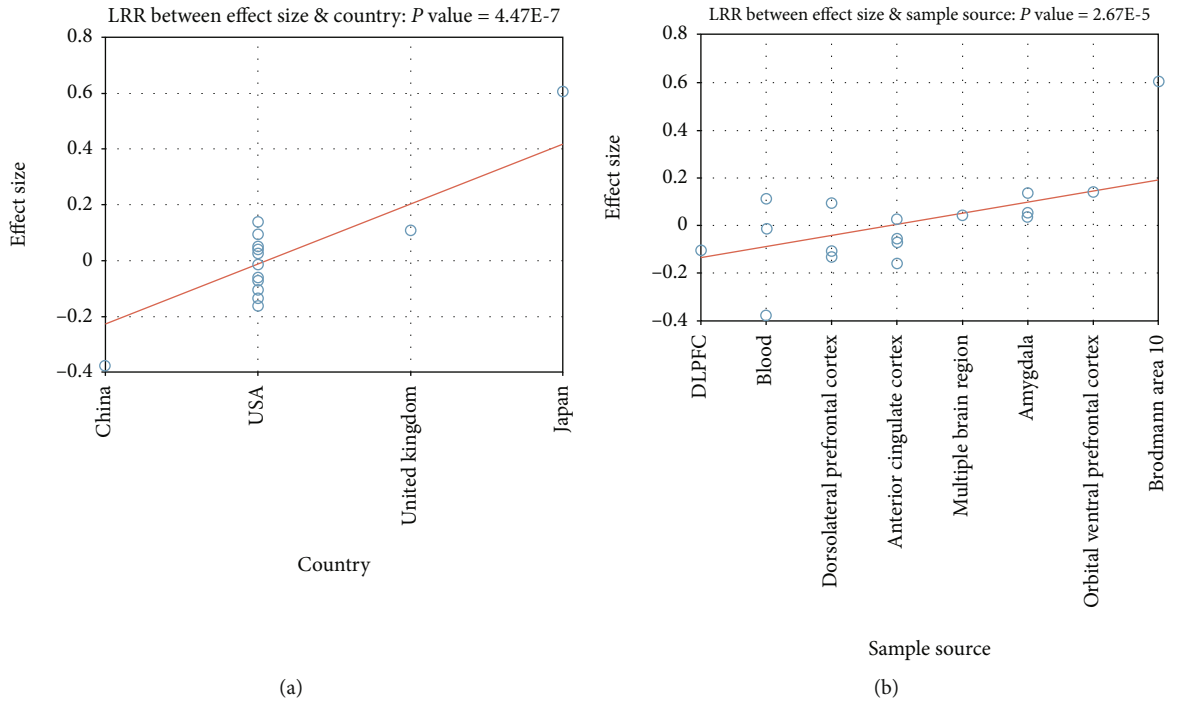


Figure 3: Multiple linear regression analysis results for the influential factors of PPARD expression in the cases of major depressive disorder: (a) results for population regions (country); (b) results for sample source.

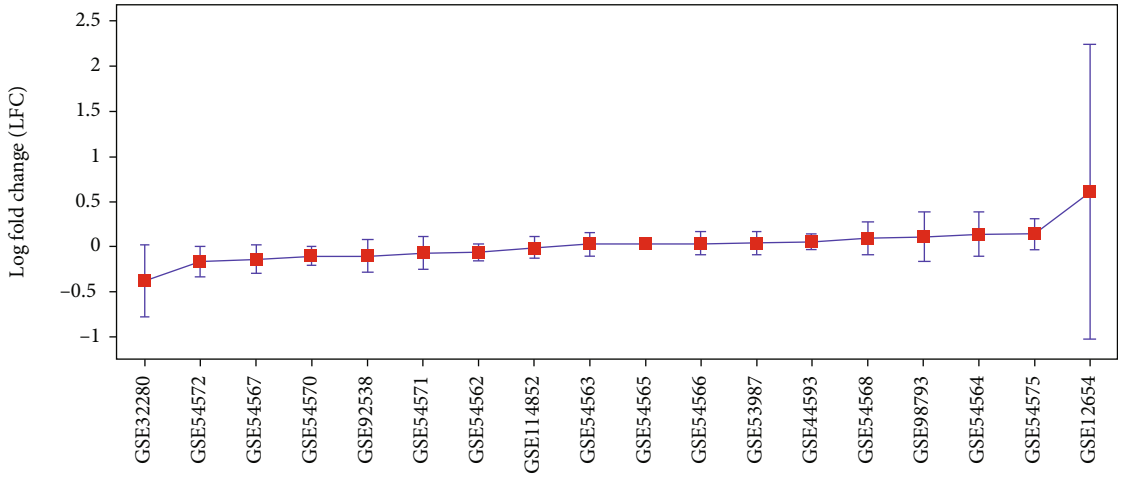


Figure 4: Error bar plot of the within-study variance of the PPARD expression among 18 major dispersive disorder RNA expression datasets.

dataset GSE12654 that presented the highest averaged expression levels (LFC = 0.60) also demonstrated the most significant within-study variance (STD = 1.63). For more details of these results, please refer to ExpressionOfPPARD in the Supplementary Materials. Our results indicated that the variation might partially cause the overall nonobvious expression changes of PPARD in MDD patients among samples within each study.

## 4. Discussion

In this study, we explored the possible relationship between PPARD and MDD through literature-based network analysis and RNA expression variation analysis of PPARD in the cases of MDD. Moreover, we employed multiple linear regression analysis and heterogeneity analysis to study the potential, influential factors of PPARD expression in the cases of MDD. Coexpression analysis between PPARD and its driven genes was conducted to provide partial validation of the PPARD-driven MDD regulating pathway. The literature-based pathway in Figure 1 supports the hypothesis that PPARD might be involved in the pathogenesis of MDD by regulating cytokine-related signaling pathways. However, our results also demonstrated the variation of PPARD expressions in the cases of MDD, which may be influenced by multiple factors, including sample postulation regions and sample sources. These results suggested that PPARD might be a regulator rather than a biomarker for the pathological development of MDD.

Firstly, literature-based network analysis showed that PPARD might influence multiple molecules that functionally regulate MDD, mostly in a beneficial way (Figure 1). Our results were consistent with previous studies that PPARG plays a crucial role in regulating depression and depressive behaviors [11, 12]. Most noticeably, PPARG was shown to inhibit multiple cytokine signaling pathways, which have been demonstrated to play an important role in the pathophysiology of MDD [15]. On the one hand, PPARD activation blocks the synthesis of inflammatory cytokines, including IL1$\beta$, IL6, and TNF$\alpha$ [16], which explains the fact that PPARD agonists downregulate the expression of these cytokines [17]. On the other hand, serum TNF$\alpha$, IL6, and IL1$\beta$ were implicated as important factors in the psychopathology of acute-phase MDD [18], which were found to stimulate behavioral changes of MDD [19]. These findings support the PPARD-cytokine signaling-MDD pathways, where increased expression of PPARD plays an inhibitive role in MDD.

Moreover, the pathway analysis also revealed that PPARD inhibits two small molecules that were the promoters of MDD, namely, free oxygen radicals (ROS) and glutamate (Figure 1). Activation of PPARD was found to counteract angiotensin II-induced ROS generation and modulates glutamate release [20–22], which have been suggested to play essential roles in the pathophysiology of MDD [23, 24]. PPARD activation also stimulates the biosynthesis of tetrahydrobiopterin [25], which was implicated to play a role in clinical depression [26]. These findings suggested additional pathways where PPARD plays beneficial functions in the pathological development of MDD.

However, our pathway analysis also revealed that PPARD activation promotes the nitric oxide (NO) formation and ceramide synthesis [27, 28], which were found to play important roles in the neurobiology of major depression [29, 30]. These findings suggested the complicity of the relationship between PPPARD and MDD.

Coexpression analysis suggested that decreased expression of PPARD in MDD patients might lead to elevated IL6 expression, while overexpression of PPARD could suppress the expression of TNF. Both IL6 and TNF encode cytokines that have been shown to play a key role in the pathogenesis of MDD [31]. These findings support a potential PPARD → -cytokine → MDD signaling pathway that has been identified through literature data mining (Figure 1).

Expression data analysis showed that PPARD only demonstrated mild variations among 18 different MDD datasets (LFC = −0.38 to 0.61), with 55.56% of studies presenting overexpression and 44.44% studies showing reduced expression. As the datasets were collected from four different countries

and eight different sample sources and using six different platforms, our study results may well represent different cases of MDD. Our results suggested that PPARD might not be a biomarker for the pathological development of MDD. Although the deficiency of PPARD might lead to depression-like behaviors and promote the development of MDD, it may not naturally happen in the majority of MDD patients. We presented the details of the PPAR expression in ExpressionOfPPARD in the Supplementary Materials.

MLR analysis showed that the population region (country) and sample source were significant, influential factors ($p = 4.47E-07$ and $2.67E-05$, respectively) of PPARD expression levels in the case of MDD. Moreover, a heterogeneity analysis indicated that significant within-study variance might exist among individual MDD patients (see Figure 4), which is worthy of further study. However, due to the lack of clinical information of the 18 expression datasets, the related analysis was not conducted in this study.

This study has several limitations that need further investigation. First, the pathways built (Figure 1) were based on previous studies. Although coexpression analysis provided partial validation of the pathway, biology experiments are needed to test the relationships identified. Second, more clinical parameters (e.g., age, gender, disease stage, and drug status) should be tested regarding their influence on MDD expression variation.

## 5. Conclusion

This study was among the first studies to explore the relationship between PPARD and MDD. The literature-based pathway built here supported a potential PPARD → MDD relationship that is worthy of further investigation. However, PPARD might not be a biomarker for MDD at the gene expression level.

## Data Availability

The data used or analyzed during the current study are available from the corresponding author on a reasonable request.

## Conflicts of Interest

The authors declare that there is no conflict of interest regarding the publication of this paper.

## Acknowledgments

This work was supported by the Science and Technology Support Program of Sichuan (Grant No. 2019YFS0218)

## Supplementary Materials

The supplementary materials is a multiworksheet Excel file that contains additional results described as follows. (1) Ref4Pathway: reference information for the network built in Figure 1. (2) ExpressionOfPPARD: the expression of PPARD in 18 MDD RNA expression datasets and the coexpression analysis between PPARD and IL6 and TNF. (3) MLR_Results: the multiple linear regression analysis results for the potential factors influencing the PPARD expression in MDD patients. The Excel file is available online at http://www.gousinfo.com/database/Data_Genetic/PPARD_MDD.xls. *(Supplementary Materials)*

## References

[1] K. P. Lesch, "Gene-environment interaction and the genetics of depression," *Journal of Psychiatry & Neuroscience*, vol. 29, no. 3, pp. 174–184, 2004.

[2] T. Nabeshima and H. C. Kim, "Involvement of genetic and environmental factors in the onset of depression," *Experimental Neurobiology*, vol. 22, no. 4, pp. 235–243, 2013.

[3] N. Lopizzo, L. Bocchio Chiavetto, N. Cattane et al., "Gene-Environment interaction in major depression: focus on experience-dependent biological systems," *Frontiers in Psychiatry*, vol. 6, p. 68, 2015.

[4] V. Krishnan and E. J. Nestler, "The molecular neurobiology of depression," *Nature*, vol. 455, no. 7215, pp. 894–902, 2008.

[5] Y. Chida, M. Hamer, J. Wardle, and A. Steptoe, "Do stress-related psychosocial factors contribute to cancer incidence and survival?," *Nature Clinical Practice. Oncology*, vol. 5, no. 8, pp. 466–475, 2008.

[6] M. von Korff, P. Crane, M. Lane et al., "Chronic spinal pain and physical-mental comorbidity in the United States: results from the national comorbidity survey replication," *Pain*, vol. 113, no. 3, pp. 331–339, 2005.

[7] J. M. Loftis and P. Hauser, "The phenomenology and treatment of interferon-induced depression," *Journal of Affective Disorders*, vol. 82, no. 2, pp. 175–190, 2004.

[8] K. R. Dunning, D. L. Russell, and R. L. Robker, "Lipids and oocyte developmental competence: the role of fatty acids and $\beta$-oxidation," *Reproduction*, vol. 148, no. 1, pp. R15–R27, 2014.

[9] J. W. Woods, M. Tanen, D. J. Figueroa et al., "Localization of PPAR$\delta$ in murine central nervous system: expression in oligodendrocytes and neurons," *Brain Research*, vol. 975, no. 1-2, pp. 10–21, 2003.

[10] H. Higashiyama, A. N. Billin, Y. Okamoto, M. Kinoshita, and S. Asano, "Expression profiling of peroxisome proliferator-activated receptor-delta (PPAR-delta) in mouse tissues using tissue microarray," *Histochemistry and Cell Biology*, vol. 127, no. 5, pp. 485–494, 2007.

[11] M. J. Ji, X. B. Yu, Z. L. Mei et al., "Hippocampal PPAR$\delta$ overexpression or activation represses stress-induced depressive behaviors and enhances neurogenesis," *International Journal of Neuropsychopharmacology*, vol. 19, no. 1, p. pyv083, 2016.

[12] F. Chen, X. Yu, G. Meng et al., "Hippocampal genetic knockdown of PPAR$\delta$ causes depression-like behaviors and neurogenesis suppression," *The International Journal of Neuropsychopharmacology*, vol. 22, no. 6, pp. 372–382, 2019.

[13] A. Yuryev, Z. Mulyukov, E. Kotelnikova et al., "Automatic pathway building in biological association networks," *BMC Bioinformatics*, vol. 7, no. 1, p. 171, 2006.

[14] M. Borenstein, L. V. Hedges, J. P. Higgins, and H. R. Rothstein, "A basic introduction to fixed-effect and random-effects models for meta-analysis," *Research Synthesis Methods*, vol. 1, no. 2, pp. 97–111, 2010.

[15] T. Pace, "101. Brain molecular mechanisms of glucocorticoid resistance," *PsychoNeuroImmunology Research Society Annual Meeting 2009*, vol. 23, p. S53, 2009.

[16] R. Shawky, T. M. Kamal, S. Raafat, and G. H. el Nady, "Genotyping of *PPAR- γ* gene polymorphism in Egyptian neonates affected with sepsis disease and its severity," *Egyptian Journal of Medical Human Genetics*, vol. 19, no. 3, pp. 215–220, 2018.

[17] M. Altinoz, İ. Elmaci, A. Hacimuftuoglu, A. Ozpinar, E. Hacker, and A. Ozpinar, "PPARδ and its ligand erucic acid may act anti-tumoral, neuroprotective, and myelin protective in neuroblastoma, glioblastoma, and Parkinson's disease," *Molecular Aspects of Medicine*, vol. 78, p. 100871, 2021.

[18] T. L. Huang and C. T. Lee, "T-helper 1/T-helper 2 cytokine imbalance and clinical phenotypes of acute-phase major depression," *Psychiatry and Clinical Neurosciences*, vol. 61, no. 4, pp. 415–420, 2007.

[19] J. Ahrén-Moonga, M. Lekander, N. von Blixen, J. Rönnelid, S. Holmgren, and B. af Klinteberg, "Levels of tumour necrosis factor-alpha and interleukin-6 in severely ill patients with eating disorders," *Neuropsychobiology*, vol. 63, no. 1, pp. 8–14, 2011.

[20] J. S. Hwang, S. Y. Eun, S. A. Ham et al., "PPARδ modulates oxLDL-induced apoptosis of vascular smooth muscle cells through a TGF-β/FAK signaling axis," *The International Journal of Biochemistry & Cell Biology*, vol. 62, pp. 54–61, 2015.

[21] M. Y. Ahn, S. A. Ham, T. Yoo et al., "Ligand-activated peroxisome proliferator-activated receptor δ attenuates vascular oxidative stress by inhibiting thrombospondin-1 expression," *Journal of Vascular Research*, vol. 55, no. 2, pp. 75–86, 2018.

[22] E. Challet, I. Denis, V. Rochet et al., "The role of PPARβ/δ in the regulation of glutamatergic signaling in the hamster suprachiasmatic nucleus," *Cellular and Molecular Life Sciences*, vol. 70, no. 11, pp. 2003–2014, 2013.

[23] M. Bilici, H. Efe, M. A. Köroğlu, H. A. Uydu, M. Bekaroğlu, and O. Değer, "Antioxidative enzyme activities and lipid peroxidation in major depression: alterations by antidepressant treatments," *Journal of Affective Disorders*, vol. 64, no. 1, pp. 43–51, 2001.

[24] K. Hashimoto, "Emerging role of glutamate in the pathophysiology of major depressive disorder," *Brain Research Reviews*, vol. 61, no. 2, pp. 105–123, 2009.

[25] D. D. Chen, L. Y. Chen, J. B. Xie et al., "Tetrahydrobiopterin regulation of eNOS redox function," *Current Pharmaceutical Design*, vol. 20, no. 22, pp. 3554–3562, 2014.

[26] A. L. Fu, S. P. Wu, Z. H. Dong, and M. J. Sun, "A novel therapeutic approach to depression via supplement with tyrosine hydroxylase," *Biochemical and Biophysical Research Communications*, vol. 351, no. 1, pp. 140–145, 2006.

[27] Y. Mizutani, H. Sun, Y. Ohno et al., "Cooperative synthesis of ultra long-chain fatty acid and ceramide during keratinocyte differentiation," *PLoS One*, vol. 8, no. 6, article e67317, 2013.

[28] C. Y. Shih, M. H. Lin, H. C. Fan, F. C. Chen, and T. C. Chou, "Mechanisms of antiplatelet activity of nifedipine," *Journal of Hypertension*, vol. 32, no. 1, pp. 181–192, 2014.

[29] A. Dhir and S. K. Kulkarni, "Antidepressant-like effect of 1-(7-methoxy-2-methyl-1,2,3,4-tetrahydro-isoquinolin-4-YL)-cyclohexanol, a putative trace amine receptor ligand involves l-arginine-nitric oxide-cyclic guanosine monophosphate pathway," *Neuroscience Letters*, vol. 503, no. 2, pp. 120–124, 2011.

[30] A. Gulbins, H. Grassmé, R. Hoehn et al., "Regulation of neuronal stem cell proliferation in the hippocampus by endothelial ceramide," *Cellular Physiology and Biochemistry*, vol. 39, no. 2, pp. 790–801, 2016.

[31] Y. Liu, "Interleukin (IL)-6, tumour necrosis factor alpha (TNF-α) and soluble interleukin-2 receptors (sIL-2R) are elevated in patients with major depressive disorder: a meta-analysis and meta-regression," *Journal of Affective Disorders*, vol. 139, no. 3, pp. 230–239, 2012.